NMRF/TR/01/2019

सत्यमेव जयते

TECHNICAL REPORT

Implementation of Unified Model based Global Coupled Modelling System at NCMRWF

Ankur Gupta, Ashis K Mitra and E.N. Rajagopal

January, 2019

National Centre for Medium Range Weather Forecasting
Ministry of Earth Sciences, Government of India
A-50, Sector-62, Noida-201 309, INDIA

Implementation of Unified Model based Global Coupled Modelling System at NCMRWF

Ankur Gupta, Ashis K Mitra and E.N. Rajagopal

January, 2019

National Centre for Medium Range Weather Forecasting
Ministry of Earth Sciences
A-50, Sector 62, Noida-201309, INDIA

Ministry of Earth Sciences
National Centre for Medium Range Weather Forecasting
Document Control Data Sheet

1	Name of the Institute	National Centre for Medium Range Weather Forecasting
2	Document Number	NMRF/TR/01/2019
3	Date of publication	January, 2019
4	Title of the document	Implementation of Unified Model based Global Coupled Modelling System at NCMRWF
5	Type of Document	Technical Report
6	No.of pages & Figures	52 pages including 18 figures
7	Number of References	36
8	Author (S)	Ankur Gupta, Ashis K Mitra and E.N. Rajagopal
9	Originating Unit	NCMRWF
10	Abstract	All components of the earth system like atmosphere, land-surface, ocean and sea-ice play important roles in simulating realistic weather-climate across scale. Over the last few years, NCMRWF has developed a complete state of the art weather prediction system which consists of advanced observation processing, assimilation and forecast systems. Till recently, the prediction models at NCMRWF were atmospheric-only models with a fixed lower boundary condition over ocean. Recently, NCMRWF has implemented a coupled weather-climate model with a full dynamical ocean and sea-ice components to better represent the time evolution of lower boundary condition and associated feedback from air-sea interactions. This work is in the direction of implementing a seamless modeling framework at NCMRWF in which same dynamical core is used across scales. This report provides technical details of the coupled model implementation on Bhaskara HPC System at NCMRWF along with the description of components of the model. The coupled system was configured with a 65km atmosphere with 85 vertical levels extending up to stratosphere (85 km), and a 25 km ocean with 75 vertical levels. The coupling frequency is kept at one hour. The coupled model simulations at NWP time-scale for 2017 monsoon are discussed including comparisons with high-resolution stand-alone atmospheric and ocean models. The coupled model was run up to day-15 on real-time basis, and we analyze the results for monsoon 2017 season. It is noted that the large-scale features of monsoon as seen in 850, 500, 200 hPa winds and rainfall over Indian region are simulated well by the coupled model. The oceanic features like SST, SSS and surface currents are also represented well. The coupled model also captures well the features related to sea-ice in the Polar Regions. The simulated features from the coupled model also

		compares well with the analysis beyond Day-9 and up to Day-15. This coupled model system will be used at NCMRWF for days-to-season forecasts by varying its resolution and configurations.
11	Security classification	Non-Secure
12	Distribution	Unrestricted Distribution
13	Keywords	Coupled model, seamless modelling, monsoon, sea surface temperature, sea ice concentration

Table of Contents

List of Figures

List of Tables

Abstract

All components of the earth system like atmosphere, land-surface, ocean and sea-ice play important roles in simulating realistic weather-climate across scale. Over the last few years, NCMRWF has developed a complete state of the art weather prediction system which consists of advanced observation processing, assimilation and forecast systems. Till recently, the prediction models at NCMRWF were atmospheric-only models with a fixed lower boundary condition over ocean. Recently, NCMRWF has implemented a coupled weather-climate model with a full dynamical ocean and sea-ice components to better represent the time evolution of lower boundary condition and associated feedback from air-sea interactions. This work is in the direction of implementing a seamless modeling framework at NCMRWF in which same dynamical core is used across scales. This report provides technical details of the coupled model implementation on Bhaskara HPC System at NCMRWF along with the description of components of the model. The coupled system was configured with a 65km atmosphere with 85 vertical levels extending up to stratosphere (85 km), and a 25 km ocean with 75 vertical levels. The coupling frequency is kept at one hour. The coupled model simulations at NWP time-scale for 2017 monsoon are discussed including comparisons with high-resolution stand-alone atmospheric and ocean models. The coupled model was run up to day-15 on real-time basis, and we analyze the results for monsoon 2017 season. It is noted that the large-scale features of monsoon as seen in 850, 500, 200 hPa winds and rainfall over Indian region are simulated well by the coupled model. The oceanic features like SST, SSS and surface currents are also represented well. The coupled model also captures well the features related to sea-ice in the Polar Regions. The simulated features from the coupled model also compares well with the analysis beyond Day-9 and up to Day-15. This coupled model system will be used at NCMRWF for days-to-season forecasts by varying its resolution and configurations.

1 Introduction

A state-of-the-art weather-climate prediction system has components like atmosphere, land, ocean, and sea-ice. Each of the components along with their simultaneous interactions and feed-back mechanisms produce realistic prediction across timescales. For a long time, however, efforts in numerical weather prediction were based on models with atmospheric dynamics only. Lower boundary in these models was either represented by fixed sea surface temperatures (SSTs) or persistent SST anomalies. Historically, the role of coupled processes on the mean state of atmosphere and its variability at seasonal and climate scales was better understood than at sub-seasonal scales. Several modes of climate variability have been understood as inherently coupled air-ocean interaction phenomenon, such as: Pacific Decadal Oscillations (PDO), El-Nino-Southern Oscillations (ENSO), etc. At seasonal scale, the dynamic predictability of the planetary scale phenomenon, such as monsoons, has been shown to depend on surface boundary conditions (Charney and Shukla, 1981). Thus, the developments in coupled modeling were motivated by the need to accurately simulate the mean state and long-range variability of ocean–atmosphere system.

The effect of coupling at short to medium range was often overlooked mainly due to the dominant modes of variability in ocean being at longer time scales and also due to unavailability of real-time ocean data-assimilation systems. However, the representation of time-varying lower boundary conditions has been found to be useful in simulating the sub-seasonal variability of atmosphere (Demott, Klingaman and Woolnough, 2015). Recent studies have also demonstrated the importance of coupling for monsoon prediction at sub-seasonal scale. The phase and amplitude of monsoon intra-seasonal oscillations (MISO) are captured better in coupled models (Abhilash et al., 2014; Sarkar et al., 2018). Positive impact of coupling is even seen on Day-10 to Day-15 forecast of 850 hPa temperatures (Vitart et al., 2008). In recent years, due to the availability of state-of-art ocean assimilation systems, ocean assimilation and short to medium range forecasting has been realized at many ocean operational centers in India and elsewhere (Bell et al., 2009). With the improvements in model physics, dynamics and representation of lower-boundary condition, the skill of models in prediction at sub-seasonal time scales has improved particularly in the last decade. Availability of high performance computing resources was also another handicap for modeling centers in India, which has improved now.

Recognizing the importance of coupled processes and improvement in skill across-scales due to representation of air-sea interaction in models, many centers such as European Center for Medium-Range Weather Forecasts (ECMWF), National Ocean and Atmosphere Administration's (NOAA) Climate Prediction Centre (CPC),Japan Meteorological Agency (JMA), Australian Bureau of Meteorology Research Centre (BMRC), Indian Institute of Tropical Meteorology (IITM) etc. have started using coupled models for weather-climate prediction. In May 2010, NCMRWF implemented a 4D-VAR atmospheric data assimilation system, and Unified Model based forecast system (NCUM) was made operational in March 2012. Motivated by developments in the field of coupled seamless modeling, a state-of-the-art ocean data assimilation has been implemented in June 2016 at NCMRWF. Following winter, a coupled model suite was tested, and beginning March, 2017, real-time runs of coupled model was started at medium range time-scale (up to 15 days runs). The coupled system was configured with a 65km resolution atmosphere with 85 vertical levels extending up to stratosphere (85 km) and a 25 km resolution ocean with 75 vertical levels. This report describes the particulars of the configurations used, brief descriptions of different model components and technical details of implementation of coupled model suite in Bhaskara HPC (350TF IBM iDataPlex HPC system).This work is aimed at implementing a seamless coupled modeling system at NCMRWF (Mitra et al. 2013) for prediction from days to season.

2 Global Coupled Model configuration

NCMRWF works in close collaboration with UK Met Office and the Unified Model (UM) Partnership. The UM is used with different configurations for numerical modeling at weather, seasonal and climate scales. The earlier configurations GloSea5-GA3 for seasonal and HadGEM2-AO for climate scales are documented in (Maclachlan et al., 2015) and (Martin et al., 2011) respectively. During March 2014, a configuration named Global Coupled model 2.0 (GC2) was tested, which aimed to use similar configuration at all scales from days-to-season in a seamless approach (Williams et al., 2015).The GC2 configuration is defined by the scientific configurations of each of the component models and the ways in which these components are coupled together using a coupler. These configurations of each component models are documented by (Walters et al., 2017) for Global Atmosphere 6.0 (GA6.0) and Global Land 6.0 (GL6.0), (Megann et al., 2014) for Global Ocean 5.0 (GO5.0), and (Rae et al., 2015) for Global

Sea Ice 6.0 (GSI6.0). All of these components show noteworthy improvements over their predecessors. The GC2 configuration has been extensively tested and documented by (Williams et al., 2015). At NCMRWF GC2 configuration has been implemented for initial use in coupled modeling. The ocean coupling frequency is set at every one hour.

2.1 Global Atmosphere: UM

The Unified Model (UM) is used as the atmospheric model in the coupled configuration.

Grid and Resolution

The resolution of the model is defined by the number N which represents number of 2 grid-point waves that can be represented by the model, thus having $2N$ and $1.5N$ grid points in zonal and meridional direction, respectively. The configuration used here is at$N216$resolution which is around 65km in the mid-latitudes. Arakawa C-grid staggerring has been used for horizontal discretization, while Charney-Phillips staggering has been used for vertical discretization in a terrain-following hybrid height coordinate system. The GC2 configuration uses 85 levels in vertical reaching a height of 85 km. This is different from the operational atmospheric model (NCUM), which has lower model lid at 80 km with 70 levels. Both GC2 and currently operational atmospheric model has same 50 levels below 18 km, but GC2 has higher resolution in stratosphere.

Dynamical Core

The dynamical core of the model, called ENDGame (Even Newer Dynamics for General atmospheric modeling of the environment)(Wood et al., 2014), is based on the semi-implicit semi-Lagrangian (SISL) formulation to solve for the non-hydrostatic, fully compressible deep-atmosphere in terms of seven primary prognostic variables: winds in three dimensions, virtual dry potential temperature, Exner pressure and dry density; as well as moisture and cloud fields and other atmospheric loadings. The introduction of SISL in an earlier dynamical core, New Dynamics (ND) has allowed solving virtually un-approximated set of equations in a time constrained by operational procedures. Compared to ND, ENDGame has improved accuracy, scalability and stability of the model. A nested approach is used in ENDGame in which the slow physical processes such as radiation, large-scale precipitation and gravity-wave drag are solved first; the appropriate fields are then interpolated to departure points computed using SISL; the fast physical processes such as atmospheric boundary layer, turbulence, convection and land surface coupling are then computed before applying the Helmholtz equation to estimate the increments in pressure fields at each time step. All other variables are computed using back-substitution of pressure fields. This nested solution is applied iteratively over what is called two outer loops, each with two inter-loops. Multiple iterations allowed the Coriolis and orographic terms to be solved outside the Helmholtz equation; this simplified Helmholtz equation is much more scalable and cost-effective per iteration.

The nested approach of solving linear Helmholtz equation in ENDGame also improves the stability of the model. Due to stability concerns, the semi-implicit time stepping scheme was weighted close to being fully implicit in ND with off-centering weights having value between 0.7 and 1. The improved stability of ENDGame allows the off-centering weights in the semi-implicit scheme to be0.55 which is close to that needed for second-order accuracy. Further, explicit diffusion and polar filtering are applied in ND to prevent model failures due to numerical instability. A more stable ENDGame allows discontinuation of polar filtering, which reduces the communication needs across polar processors, making the code more scalable. The stability of the model is also improved due to use of trajectory midpoint velocities over the extrapolated velocities for computing the departure points. Further, in ENDGame, continuity equation is also discretized in a semi-Lagrangian manner, which improves both the accuracy and stability of the model. Also, by moving the horizontal grid point by half a grid, ENDGame has no scalar field defined at grid singularity; no Helmholtz equation is thus solved at the poles. Fewer communications among polar processors are needed to maintain the consistency of scalar fields at the poles. In the semi-Lagrangian discretization, the transport of properties of a parcel of air is achieved by tracking back the location of parcel and interpolating its properties. This approach for transport of properties is accurate but does not conserve the property being transported. To account for this, ENDGame regains mass conservation by applying a simple mass fixer. The numerical scheme being away from fully-implicit also reduced the inherent dampening in implicit schemes. These upgrades to numerical scheme were reported to improve simulation of cyclone, intra-seasonal oscillations and Indian summer monsoon.

Atmospheric physics

The model uses extensive set of parameterization schemes to represent different physical processes:

1. The large-scale precipitation is computed using the microphysics scheme based on(Wilson and Ballard, 1999). Mass-mixing ratios of aerosols, such as ammonium sulfate, sea salt, biomass burning and fossil-fuel organic carbon provide cloud droplet number for auto-conversion. The liquid content where the number of droplets over $20\,\mu m$ is$1000 m^{-3}$, is used as minimum cloud liquid content for autoconversion to happen. The prognostic rain formulation allows 3-D advection of precipitation mass-mixing ratio. The particle size distribution is made dependent on the rain-rate.
2. Prognostic cloud fraction and prognostic condensate (PC2) scheme of (Wilson et al., 2008) is used to compute the cloud fraction, liquid-water and ice-water using prognostic variables: vapor, liquid, ice, and liquid, ice and mixed phase cloud fraction. The cloud fields are modified by the radiations, boundary layer, convection, precipitation, cloud-erosion, advection and changes in atmospheric pressure.
3. The convection scheme in the model is based on mass flux scheme of (Gregory and Rowntree, 1990) with several modifications. In particular, a convective available potential energy (CAPE) based closure is used along with representation of downdraughts and convective momentum transport.
4. The radiation scheme is based on shortwave and longwave (Edwards and Slingo, 1996).
5. At the smallest scales, roughness length for momentum is increased to account for additional stress due to sub-grid orography. On scales where buoyancy effects are important, a part of the flow is parameterized to be blocked and flow around the analytical mountains, the remainder of the flow produces mountain waves and acceleration of flow due to wave stress divergence is applied at levels where wave breaking is diagnosed. This closely follows the scheme by (Lott and Miller, 1997).
6. The effects of gravity-wave forced by convection, fronts and jets are parameterized following (Scaife et al., 2002). These involve vertical wavenumber dependent processes of waver generation, conservative propagation and dissipation. Momentum deposition in each layer is such as to match the locally evaluated saturation spectrum. This

representation of wave breaking in upper stratosphere and mesosphere leads to a more realistic tropical quasi-biennial oscillation.

7. Turbulent motions not resolved by the model at the given resolution are parameterized using (Lock et al., 2000) scheme. The heat, moisture, momentum and tracers are adiabatically mixed using first-order turbulent closure. The diffusion coefficient profiles (K profiles) are specified for both surface sources (surface heating and wind shear) and cloud-top sources (radiative and evaporative cooling) of turbulence for unstable boundary layers. For stable boundary layers local Richardson number based scheme of (Smith, 1990) is used.

2.2 Global Land: JULES

The land surface and hydrology model in GC2 is based on Joint United Kingdom Land Environment Simulator (JULES)(Best et al., 2011)and is tightly coupled to the atmospheric model. Both land and atmospheric model uses same grid. The land model parameterizes the exchange of heat and momentum fluxes between land and atmosphere. Each land point is represented by a total of 9 types of vegetated and non-vegetated surface. Surface similarity theory is used to compute the surface fluxes separately on each tile. The similarity functions are different in stable and unstable conditions and take into account the boundary layer and deep convective gustiness. Four vertical soil levels are defined in GL 6.0 for computation of heat and water balances in each layer. Topography-based hydrological model TOPMODEL is used to represent the rainfall-runoff relation and simulates infiltration-excess overland flow, saturation overland flow, infiltration, ex-filtration, subsurface flow, evapo-transpiration and an interactive water table. The surface runoff is produces as excess of water balance which is routed to rivers using a river routing scheme. An advection-based Total Runoff Integrating Pathways (TRIP) model is used for routing the surface runoff accumulated over 3 hours on a $1^o x 1^o$ grid. The hydrological model, TOPMODEL, in combination with the river routing scheme, TRIP, thus computes the water balance over the land and provides freshwater forcing to the ocean. The freshwater forcing is an important coupled process between the land-ocean-atmosphere system which changes the ocean stratification and upper layer heat budget.

2.3 Global Ocean: NEMO

The GO5.0 configuration used in GC2 is jointly developed by the Met Office and National Oceanography Centre, supported by National Environment Research Council (NERC), UK to provide a modeling framework across timescales, from short-range forecasting to climate prediction, in a seamless approach. The configuration uses the Nucleus for European Modeling of the Ocean (NEMO) version 3.4 as the ocean model with some patches to code applied to couple with UM and JULES executable using OASIS coupler. The base NEMO model was downloaded from the NEMO consortium web site (https://www.nemo-ocean.eu/)

Grid and Resolution

The ocean and sea-ice models are defined at an eddy-permitting resolution of $1/4^o$ on a tripolar orthogonal curvilinear grid called ORCA025. South of 20N it is an isotropic Mercator grid, i.e. same zonal and meridional grid spacing. North of 20N, the set of mesh parallels used is a series of embedded ellipses which foci are the two mesh north poles (107^o W and 73^o E). The gives an effective grid size of ~27.8 km at the equator but decreasing towards the poles. The model has 75 z-coordinate vertical levels with the thickness of layers increasing from 1m near the surface to 200m at 6000m. The bathymetry used in GO5.0 is DRAKKAR v3.3 which is an update from an earlier version in using 1-minute resolution ETOPO1 data set (Amante and Eakins, 2009) with additional information in coastal regions from GEBCO (General Bathymetric Chart of the Oceans; IOC, IHO, and BODC In, 2003).

Ocean dynamics

The model solves the prognostic equations in their vector invariant form in which Coriolis and advection terms are decomposed into vorticity, kinetic energy and vertical advection terms. Other forces include horizontal and surface pressure gradients, and contributions from lateral and vertical diffusion. The generalized Arakawa C-grid is used to represent the variables in which the scalars are located at cell's center and vectors are located at the center of faces of the cell. The spatial discretization is based on centered second-order finite difference approximation. The vorticity term is discretized using so called EEN scheme which conserves both the potential enstrophy of horizontal non-divergent flow and horizontal kinetic energy. For diffusive terms, a backward (or implicit) time differencing scheme is used. Non-diffusive forcings are solved using well known leapfrog time-differencing scheme of (Mesinger and Arakawa, 1976) with some modifications. The tracers are advected using total variance dissipation scheme in which tracer at velocity points are computed using upstream value of tracer added to a weighted centered differenced value. A bi-Laplacian horizontal viscosity reducing poleward as a cubic function of maximum grid dimension is used with a value of $1.5x10^{11}\ m^4 s^{-1}$ at the equator. A quadratic bottom friction is used in the configuration with increased coefficient in the Indonesian Throughflow, Denmark Strait and Bab-el-Mandeb regions. Surface layer height is a diagnostic variable and is computed by integrating the linear surface kinematic condition. Explicit filtering of fast gravity waves is implemented to allow reasonable time step for model integrations.

Ocean physics

Diapycnal mixing is parameterized using a modified version of (Gaspar, Grégoris, and Lefevre, 1990) turbulent kinetic energy scheme. The effect of energy transfer from barotropic tides to internal tides and internal tide breaking due to rough topography is parameterized based on (Simmons et al., 2004), with enhanced tidal dissipation efficiency in the region of Indonesian Throughflow to account for trapped internal waves in the Indonesian Archipelago. An advective and diffusive bottom boundary layer scheme based on (Beckmann and Döscher, 1997) is also included.

2.4 Global Sea Ice: CICE

GSI 6.0 sea ice configuration is used in the GC2 implementation (Rae et al., 2015). GSI uses the Los Alamos National Laboratory sea ice model (CICE) version 4.1 as the sea ice model. Five categories of seaice based on thickness are included in GO5.0 with elastic-viscous-plastic ice dynamics of (Hunke and Dukowicz, 1997) and energy-conserving thermodynamics of (Bitz and Lipscomb, 1999).

2.5 The coupling framework: OASIS3.0

The components of the earth system in the GC2 configuration are each represented by a separate model: the UM for the atmosphere, the JULES for the land, NEMO for the ocean, and the CICE for the sea-ice. Each of the models requires initial, boundary and forcing fields for numerical integrations. These are provided by fields such as SSTs etc. as lower boundary condition for the atmosphere and heat, momentum and fresh-water fluxes etc. as forcings for the ocean and sea-ice models. The fields are initialized using appropriate initial conditions. The components models of the coupled system allow these fields to be simulated as heat and freshwater fluxes, etc. in the atmospheric model and SSTs etc. in the ocean model. This makes the component models depend on each other and requires the fields to be exchanged at a predetermined coupling frequency. However, the grid structure and resolutions of the component models could be different. All component models in GC2 uses Arakawa C-grid for horizontal discretization with the exception of CICE velocities defined on Arakawa B-grid. Further, while the atmospheric model has a regular lat-lon grid with resolution of ~60km at mid-latitudes, ocean model has tripolar grid with a resolution of ~25 km near equator. The difference in grid structure requires a set of intermediary routines to remap the fields from one model grid to another. In GC2, this is achieved by relying on version 3 of OASIS coupler.

Here, the atmosphere and land models are compiled into a single executable and the ocean and sea-ice models are compiled into another executable. However, the heat and momentum fluxes over land, ocean and sea-ice are all computed in land surface model only. The OASIS coupler handles the exchange and interpolation of fields between the two executables at a frequency of 1 hour, while the fields shared by component models of a single executable are passed by either subroutines arguments or accessing shared data arrays.

2.5.1 Interpolation method used in exchange of fields

A total of 38 fields are exchanged between the component models.

1. Fields with first order conservative remapping with ‘Destarea’: 10-m wind speed, freshwater and heat fluxes are computed in the atmospheric model and passed to ocean model. A first order conservative remapping normalized using destination area is used for these fields.
2. Fields with second order conservative remapping with ‘Fracarea’: SST, sea-ice fraction, and ice and snow thickness.
3. Fields with bilinear interpolation: ocean currents, wind-stress

In original GC2 configuration, while atmospheric fluxes are time averaged over the coupling period before sending to the ocean model to ensure conservation, ocean fields (SST, surface velocity, ice fraction, ice and snow thickness) are all instantaneous values. The implementation in current NWP configuration is based on instantaneous values for all fields to be exchanged. To account for the presence of sea ice in a single ocean grid-cell, the surface velocities of ocean-water and sea-ice are averaged according to the sea-ice fraction before being interpolated by

OASIS. Similarly, the wind stress from atmospheric model is assumed to apply equivalently to ocean-water and sea-ice. In the conservative remapping scheme, normalization of contributions from overlapping source-grid cells are done by area of the destination grid-cell in the option 'Destarea', and by the total area of the overlapped source-grid cells in 'Fracarea'. Table 1 provides list of fields exchanged from ocean to atmosphere along with the grid types involved in coupling and remapping type used for processing the exchanged fields. Similarly, Table 2 provides list of fields exchanged from atmosphere to ocean.

Table 1: List of field exchanged from ocean to atmosphere

Sl.No.	Variable Name	Grid types	Remapping type (Order,Normalization)
1	Sea Surface Temperature (K)	tor1->atm3	Conserv (Second, Fracarea)
2	Sea Ice Area Fraction (1)	tor1->atm3	Conserv (Second, Fracarea)
3	Multi-Category (ice)	tor1->atm3	Conserv (Second, Fracarea)
4	Surface Snow Amount (kg)	tor1->atm3	Conserv (Second, Fracarea)
5	Surface Grid Eastward Sea Water Velocity (m)	uor1->aum3	Bilinear
6	Surface Grid Northward Sea Water Velocity (m)	vor1->avm3	Bilinear

Table 2: List of fields exchanged from atmosphere to ocean

Sl.No.	Variable Name	Grid types exchange	Remapping type (Order,Normalization)
1	Multi-Category (Fcondtop)	atm3->tor1	Conserv (First, Destarea)
2	Multi-Category (Topmelt)	atm3->tor1	Conserv (First, Destarea)
3	Surface Downward Grid Eastward Stress (Pa)	aum3->uor1	Bilinear
4	Surface Downward Grid Northward Stress (Pa)	avm3->vor1	Bilinear
5	Surface Net Downward Shortwave Flux (W)	atm3->tor1	Conserv (First, Destarea)
6	Surface Downward Non Shortwave Heat Flux (W)	atm3->tor1	Conserv (First, Destarea)
7	Rainfall Flux (kg)	atm3->tor1	Conserv (First, Destarea)
8	Snow Fall Flux (kg)	atm3->tor1	Conserv (First, Destarea)

9	Water Evaporation Flux (1)	atm3->tor1	Conserv (First, Destarea)
10	Water Evaporation Flux Where Sea Ice (kg)	atm3->tor1	Conserv (First, Destarea)
11	Wind Speed At 10M (m)	atm3->tor1	Conserv (First, Destarea)
12	Water Flux Into Ocean From Rivers (kg)	atm3->tor1	Conserv (First, Destarea)

2.6 Model Initial, Boundary and Other Data (Startdumps and ancillary files)

NCMRWF land-atmospheric and sea-ice-ocean analysis are taken as startdumps for daily initialization of the coupled model. The atmospheric analysis is from Hybrid 4-DVardata assimilation system of NCMRWF with an in-house data pre-processing system. The data pre-processing system prepares observations in "obstore" format using the observations received at NCMRWF through GTS and various satellite data providers including NOAA-NESDIS and MOSDAC (ISRO). The data assimilation system along with details of observations assimilated is documented by (George et al., 2016). Since 2016, the assimilation system is coupled with forecast from ensemble prediction system for generating flow dependent background error in addition to climatological error(Kumar et al., 2018)). In addition to the atmospheric states, best available analyses of snow, SST, sea ice & soil moisture are part of the input dump used to initialize the atmospheric model.

The ocean and sea-ice initial conditions are produced at NCMRWF (Momin et al., 2019)using NEMOVAR which is an incremental 3D-Var data assimilation system using first guess at approximate time (FGAT) as background field(Waters et al., 2015). The system assimilates both satellite and *in situ* observations of SST, sea-level anomaly, sub-surface temperature and salinity profiles, and satellite observations of sea-ice concentrations over 1-day assimilation cycle. The ocean-sea-ice model is same in both the data assimilation system and forecast model.

Many fields including lower boundary variables (ancillary files) and distribution of aerosols and natural and anthropogenic emissions are required to initialize the model. However, such fields are either not available in the atmospheric analysis or not read from analysis file in current configuration. Climatological distribution of such fields required to initialize the atmospheric model or to be provided as external forcing are saved in static files at a given resolution. Such fields and files are termed as 'ancillary' here. These can be broadly categorized as:

1. Land parameters: orography, mean and standard deviation of the topography, land mask, land fraction and albedo
2. Vegetation parameters: fraction of surface types, leaf area index, canopy height
3. Soil parameters: saturated soil conductivity, volumetric soil moisture at saturation etc
4. River parameters: river sequence, direction and storage
5. Aerosols: sulphate (accumulation, aitken, and dissolved modes), sea salt (film and jet modes), dust (6-types), black carbon (fresh and aged)
6. Emissions: from biogenic sources, fresh, aged, in-cloud modes from biomass burning and combustion of fossil fuel (organic carbon)
7. Ozone

The ancillary data used in current configuration and their sources are described by Walters et al., 2017. Appendix A provides a complete list of ancillary files and associated fields. These are generally of two types:

1. Fields initialized from ancillary files (Table A.1)
2. Fields initialized to zero (Table A.2)

3 Technical Details of Implementation

The coupled model implementation at NCMRWF uses advanced software for scheduling of operational suite. Some of the main components of this software architecture sometimes referred as ROSE-CYLC-FCM are described below.

3.1 Cylc as the job scheduler

Cylc is a workflow engine for scheduling cycling tasks with complex inter-dependencies as well as ordinary non-cycling workflows, along with associated tasks for data collection, quality control, preprocessing, post-processing and archiving. Cylc was developed at National Institute of Water and Atmospheric Research, New Zealand for scheduling and defining the work flow for various tasks including real time processing of observations; and running inter-dependent operational weather forecast, sea state, storm surge, and catchment river models. Cylc can be used to run real-time forecast in successive cycles or concurrent cycles of hindcasts or other historical tasks.

3.2 Rose as the task manager

In addition to having a scheduler to manage dependent tasks, it is desirable for a meteorological suite to have a common way of controlling the run-time parameters needed by model executables. Rose not only complements the Cylc feature of providing a controlled environment for each task, but also has the capability to form FORTRAN-style namelists and override a user-defined set of these namelists entries. In addition, Rose comes with a suite-installer which can mirror the suite and install additional version controlled files to a remote platform where the suite is intended to be run. It uses the same suite-engine as Cylc but provides additional control over running and monitoring the suite logs.

A combined use of above Rose capabilities allows the users on a single site to run suite without any modifications and port to a different site with minimum efforts. The 'best practices' adopted during the suite-design ensure that simple suites can be merged easily with a much-complex suite and that common components between different suites can be easily merged.

Another utility Rosie allows the users to discover the suites developed by other researchers and share their suites in a version control environment to track and manager the developments by different members within a group. Both Rose and Cylc come with a Graphical User Interface (GUI) for controlling the setting described above.

3.2.1 Coupled Model Rose Suite on Met Office Science Repository Service (MOSRS)

A Rose suite is a collection of interdependent tasks. The tasks environment, resource requirement, dependencies are all defined in a file named 'suite.rc'. The coupled model rose suite (Figure 1) has following main tasks:

1. fcm_make_um: This task is used to extract and build the ocean model.
2. fcm_make_ocean: This task is used to extract, merge branches and build the atmospheric-land model.
3. retrieve_ocean: This task combines the restart files from 192 processors into a single restart file.
4. recon: This task converts the UM startdump to n216 resolution.
5. coupled: This is the main task, which runs the couple model. In particular, following environment in provided to the coupled job:

export LSF_PJL_TYPE=poe

mpirun.lsf -pgmmodel mpmd -cmdfile OASIScoupled.conf.

mpirun.lsf is a wrapper which uses the IBM Parallel Operating Environment (POE) on IBM's Load Sharing Facility (LSF) to launch the above command as:

poe -pgmmodel mpmd -cmdfile OASIScoupled.conf

The contents of the OASIScoupled.conf should specify the executable to run and number of processes to be used by the executable. In current implementation, following is used:

./oasis3:8

./toyatm:192

./toyoce:320

where toyatm, toyoce, oasis3 are to be linked to atmospheric-land, ocean-seaice and coupler executables, respectively.

6. post_process: This task achieves multiples sub-tasks:
    a. Rebuild the ocean output from 192 processors to global files
    b. Subset the ocean output to the Indian region using 'cdo' utility
    c. Upload the 15-day ocean and sea-ice forecast to FTP for sharing data with Indian National Centre for Ocean Information Services (INCOIS) and Home: National Centre for Antarctic and Ocean Research (NCAOR)
    d. Move the data to the backup directory
    e. It also does some housekeeping by removing the temporary data older than 1 day.

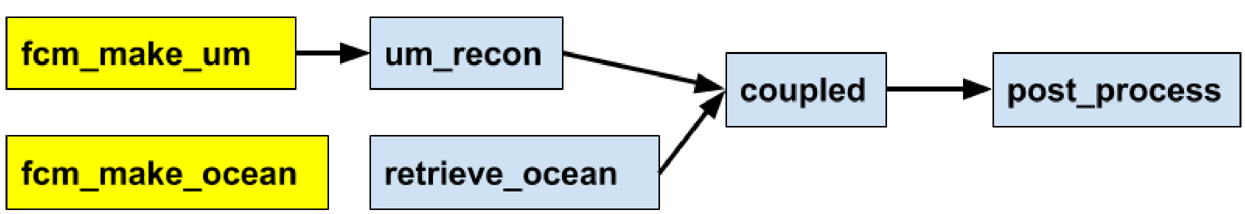

Figure 1: Schematics of the coupled suite

A working copy of the operational NWP coupled model has been committed to the MOSRS. The suite-id is: u-ab337. Several commits were done during the development phase. The revision 89583 is used for the operational version.

URL: https://code.metoffice.gov.uk/svn/roses-u/b/a/3/3/7/trunk

To run the suite, following steps may be followed on Bhaskara:

1. rosie co u-ab337
2. cd $HOME/srv/rosie/u-ab337
3. rose sutie-run

The model can be run starting any date by changing the following in the rose-suite.conf file: START_DATE="20170901T00"

END_DATE="20170901T00"

3.3 FCM as configuration manager and build automation tool

Flexible Configuration Manager (FCM) uses Subversion software for the version control of the numerical code, scripts, small control files and files containing site specific configurations required for building, installing and running the Rose based suites. It simplifies the code development and sharing by following standard working practices. FCM allows the source code to be extracted, the model to be compiled using a set of site specific configuration files. The source can be extracted from multiple repositories and multiple developmental branches and working copies. It allows incremental build and inheritance of existing build to allow faster build-run cycles during model development. By imposing a ‘coding standard’ it allows for automatic generation of dependencies, thus simplifying the build configuration files.

3.3.1 Coupled model source code

The base code used for the operational model has been taken from MOSRS at: https://code.metoffice.gov.uk/svn/um/

Version 10.2 of the code, which is at revision 7660, is merged with the following branches at the specified revision numbers:

1. branches/dev/alejandrobodas/vn10.2_COSP_McICA@8121
2. branches/dev/paulearnshaw/vn10.2_cray_seg_sizes@7697
3. branches/dev/dancopsey/vn10.2_b_regrid_swap_north@8440
4. branches/dev/joaoteixeira/vn10.2_fix_oasis3_put_bug@29833
5. branches/dev/joaoteixeira/vn10.2_ncmrwf_couple_script

The changes in the vn10.2_ncmrwf_couple_script are related to the script um-atmos. In the script default rose MPI launcher is overridden with the one specific to Load Sharing Facility (LSF) on IBM HPC.

Similarly, JULES base code is taken from MOSRS at: https://code.metoffice.gov.uk/svn/jules. The JULES revision used for the coupled model is um10.2, i.e. 1710. The radiation transfer code is hosted separately at MOSRS at: https://code.metoffice.gov.uk/svn/socrates, the same is extracted at revision um10.2: i.e. 11.

The ocean and sea-ice models are freely available from www.nemo-ocean.eu and http://oceans11.lanl.gov/trac/CICE/wiki/SourceCode respectively. NEMO 3.4 and CICE 4.1 versions are used in the operational model. The GC2 specific branches for both ocean and seaice models are obtained from Met Office. The same has been hosted as local repositories to allow NCMRWF specific changes to be tested during installation phase.

3.3.2 Build configuration

The configuration files have been adopted for IBM machine by changing the Cray-specific flags to those needed by Intel-based compilers. The atmospheric configuration files are similar to the operational UM10.2 model, with coupling related flags added to them. In particular, following has been updated in the site specific configuration files:

1. inc/ncm-ifort-mpich.cfg:

```
$flags_coupling{?} =
-I$prism_path/build/lib/mpp_io \
-I$prism_path/build/lib/psmile.MPI1 \
-I$prism_path/build/mod/oasis3.MPI1
```

2. inc/ncm-ifort-mpich.cfg:

```
$ldflags_coupling{?}=-L$prism_path/lib\
-lanaisg -lanaism -lpsmile.MPI1 \
-lfscint -lmpp_io –lscrip
```

where the prism path is:/gpfs2/home/cmprod/support/compile_oa3/lib

The ocean build configurations are adopted from existing XC 40 configurations. Some of the important changes of the ocean build configurations are summarized in Table 3.

Table 3: Changes in compilation flags for ocean model

Sl. No.	XC40-CCE	IBM-IFORT	Intel Compiler Option Short description
1	-Ovector1 -hfp0 -hflex_mp=strict	-fp-model precise	Controls the semantics of floating-point calculations. Disables optimizations that are not value-safe on floating-point data and rounds intermediate results to source-defined precision.
2	-s default64	-r8	Specifies the default KIND for real and complex declarations, constants, functions, and intrinsics. Makes default real and complex declarations, constants, functions, and intrinsics 8 bytes long. REAL declarations are treated as DOUBLE PRECISION (REAL(KIND=8)) and COMPLEX declarations are treated as DOUBLE COMPLEX (COMPLEX(KIND=8)).Real and complex constants of unspecified KIND are evaluated in double precision (KIND=8).
3	-hbyteswapio	-convert big_endian	Specifies the format of unformatted files containing numeric data. Specifies that the format will be big endian for INTEGER*1, INTEGER*2, INTEGER*4, or INTEGER*8, and big endian IEEE floating-point for REAL*4, REAL*8, REAL*16, COMPLEX*8, COMPLEX*16, or COMPLEX*32
4	-	-std03	Tells the compiler to issue compile-time messages for nonstandard language elements. Issues messages for language elements that are not standard in Fortran 2003.
5	-e m	-	modulename.mod is created by taking the name of the module and, if necessary, converting it to uppercase. The USE statement then accesses these modules while compiling.

Similar to UM, coupling specific flags have been provided in the ocean configuration files.

3.4 Libraries and dependencies

The coupled model depends on following main model-specific dependencies apart from common intel libraries to compile and run the model, and post process the model output. These dependencies are either compiled as part of GC2 installation on Bhaskara HPC, or taken from already compiled libraries from common area.

1. GCOM: GCOM is a lightweight interface to message passing layer on multi-processor machines. It provides a message passing library (MPL) module which serves as a direct

replacement of any MPI call in the application, such as UM. It allows the user to seamlessly use 32 or 64 bit precision without specifically mentioning it while calling the MPI subroutines. In the NWP coupled model GCOM 5.2 is used from a common area: /gpfs2/home/umtid/GCOM/gcom5.2/ncm_ibm_ifort_mpp/build/lib

2. netCDF and GRIB API libraries: They are used when reading the startdump in GRIB format or reading the ancillaries in netCDF format. These are currently not used as the current implementation relies on reading the UM startdump in fields file (FF) format. These libraries are nevertheless required to compile the model. The specific libraries used to compile the model are:
   /gpfs1/home/Libs/INTEL/NETCDF4/netcdf-4.2.1/lib

   /gpfs1/home/Libs/INTEL/GRIB_API/lib

3. OASIS3: It is the coupling interface used by GC2 configuration. It is also compiled outside the suite. Both the executable and libraries are needed and the paths are provided in FCM configuration files.
   /gpfs2/home/cmtest/src/prism/compile_oa3/lib
4. Rebuild_nemo: It is a small utility complied outside the rose suite. It is needed to combine the NEMO-CICE output from different processors into a single global file.
   /gpfs2/home/cmprod/support/exe/REBUILD_NEMO/rebuild_nemo

3.5 Resource Usage

The most resource intensive component of the suite is the coupled model itself. The resources used by each of the suite component task are listed below and summarized in Table 4:

1. retrieve_ocean: This task takes 10 minutes on single utility node.
2. recon: This task takes less than 5 minutes on single processor.
3. coupled:The coupled model task takes 1 hour 15 minutes to complete on 520 cores using 8 slots on each host, thus using 33 nodes in exclusive mode.

   Following directives are used while submitting the job using LSF:

```
#BSUB -a poe
#BSUB -q ensemble
#BSUB -n 520
#BSUB -R "rusage[mem=6000] span[ptile=8]"
```

#BSUB -x
#BSUB -W 03:00
In addition the racks of the supercomputer may be selected by giving following directive:

#BSUB -m ncmc07n[01-72] ncmc08n[01-72]

where ncm08n etc are the rack numbers.

4. Post_processing: The ocean model, NEMO, writes the output fields from each processor to a different file. It is left to the post-processing to combine these files into a global file. Given the high vertical resolution of the ocean model, i.e. 75 layers, and some of the high frequency ouptut, 3-hourly fluxes etc., the post processing of the ocean fields is not trivial. A utility rebuild-nemo is used for post-processing of ocean fields. The post-processing runs in background on a single utility node with run time of 50 minutes.

Table 4: Summary of resource usage

Task	Processors	Nodes	Submit Mode
retrieve_ocean	Not specified	-	background
um_recon	1	1	LSF*
coupled	520 1. UM_ATM_NPROC="192" (UM_ATM_NPROCX="8" UM_ATM_NPROCY="24") 2. NEMO_NPROC="320" (NEMO_IPROC="16" NEMO_JPROC="20") 3. PRISM_NPROC = 8	33 nodes (8 slots on each host)	LSF*
post_process	Not specified	-	background

*LSF: Load Sharing Facility

4 Discussion

4.1 Coupled Model forecast products

The atmosphere-land-ocean-seaice coupled system is simulated for 15-days as compared with 10 days for the standalone atmosphere and ocean models at NCMRWF. Complete lists of simulated variables for all three components are provided in Appendix B: Table B.1 (for land-atmosphere model), Table B.2 (for ocean model) and Table B.3 (for sea-ice model). The weather maps of 24-hourly instantaneous winds and geopotential height at 850, 700, 500, 200 hPa and daily-mean precipitation are generated in real-time and compared with the standalone atmospheric model N768L70 NCUM (Rakhi et al., 2016).At short to medium scales the advantage of coupled model can be seen particularly during the formation and intensification of tropical severe weather systems. Cyclone Titli formed as a low pressure area on 6th October, 2018 reaching to depression stage on 8th October. Figure 2 d-f shows day-5 forecast from both coupled and atmospheric only model valid on 8th October. It can be seen that the coupled model shows better organized structure and position of the depression compared to the NCUM. The cyclone quickly intensified into a very severe cyclonic storm by 10th October. Figure 2 a-c shows that while NCUM and coupled model both underestimate the intensity of the storm, but the location of the systemin coupled model forecasts is closer to the analysis. Also the NCUM shows 10-20 m/s of winds off the western coast of India associated with another storm Luban in Arabian Sea; such high intensity winds are not present in either analysis of day-7 coupled model forecast.

The product from ocean component includes plots of surface temperature, salinity and ocean currents. Also, derived parameters such as depth of 20^{0}C (D20), mixed layer depth (MLD), heat content and tropical cyclone heat potential (TCHP) are computed for visualization and analysis. On 28th May, 2017 a depression formed in central Bay of Bengal which quickly intensified into a severe cyclonic storm by 31st May. Figure 3 shows tropical cyclone heat potential (TCHP) from NCMRWF analysis and its day-5 forecast by the coupled model. TCHP is an important indicator for intensification of tropical cyclones. It is shown that the coupled model is able to predict TCHP at least 5-days in advance.

The cyclones leave a trace of their presence in the form of trailing cold sea surface temperatures (SSTs). This can be clearly seen in Figure 4 where SSTs on 10th October, 2018, just 2 days after the formation of cyclic storm Luban, are shown. A tongue of cold SSTs off the Somali coast can be seen extending northwest into the central Arabian Sea. Day-5 forecast from coupled model is also shown. It can be seen that coupled model is able to capture both the spatial structure and magnitude of cooling in the wake of the storm.

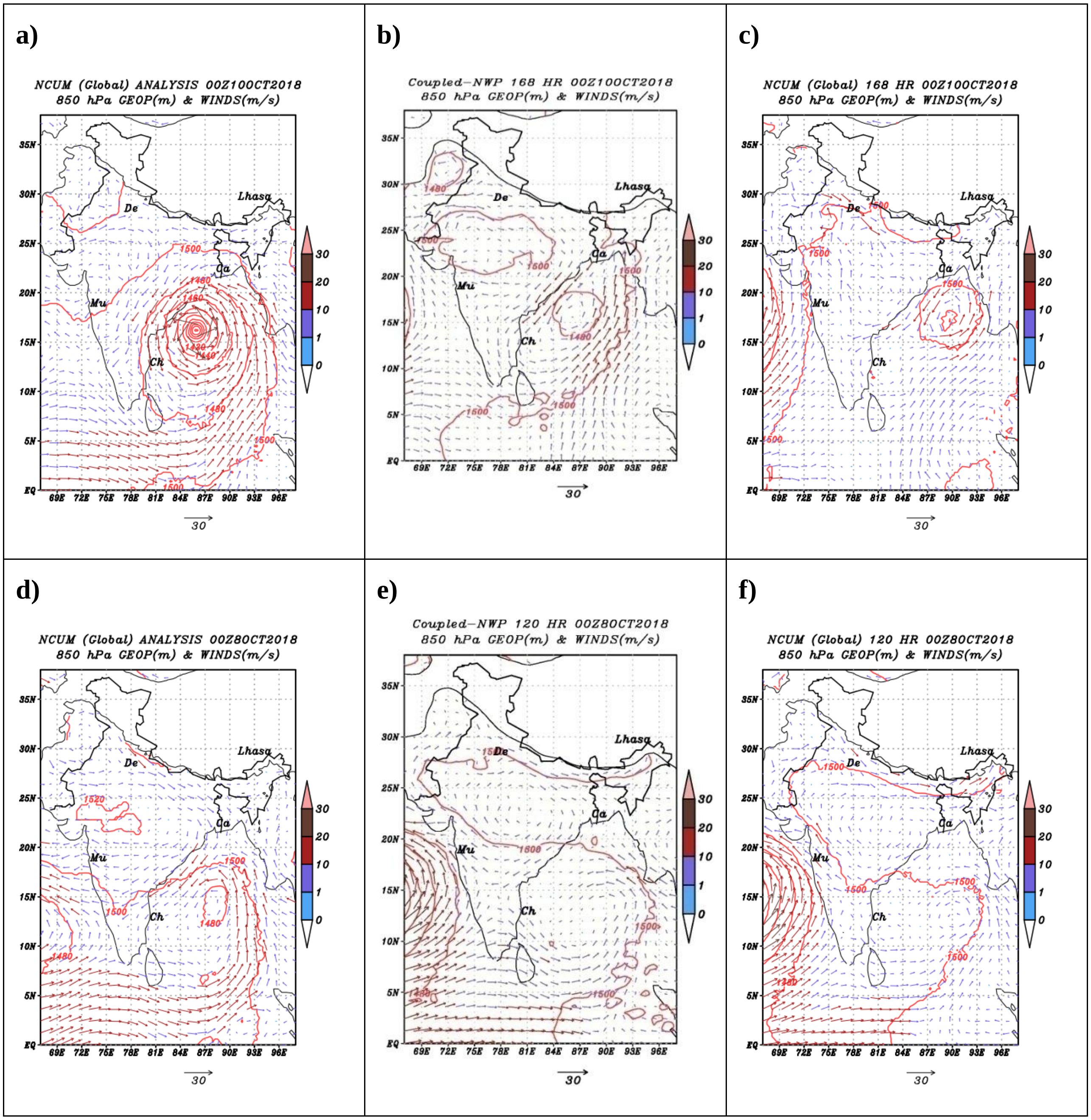

Figure 2: Geopotential height (contours) and winds (vectors) at 850 hPa height valid at 10th October, 2018 a) Analysis, b) Coupled-NWP c) Standalone-NWP

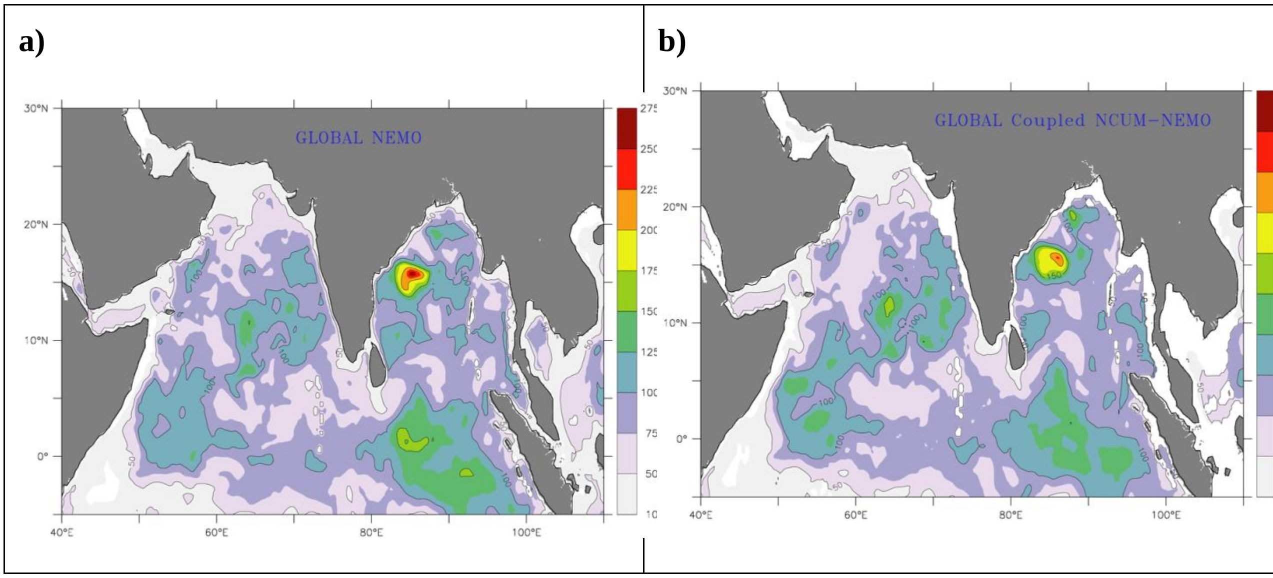

Figure 3: Tropical cyclone heat potential (KJ/cm^2) valid on 28th May 2017 derived from a) NCMRWF Ocean analysis;   b) NCMRWF Coupled Model

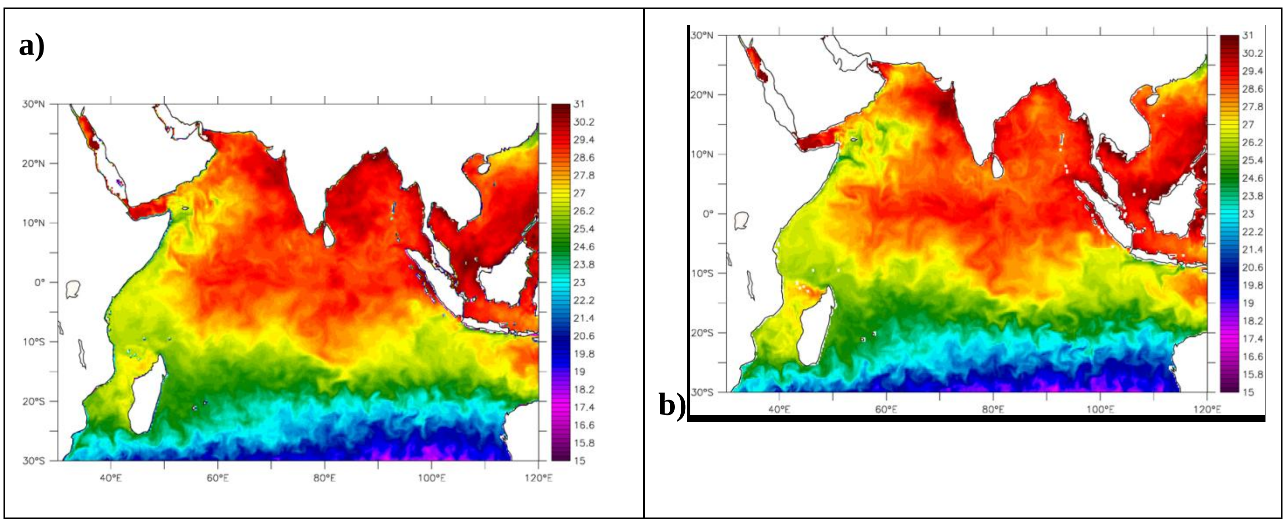

Figure 4: Sea surface temperature valid on 10th October 2018 a) NCMRWF Ocean analysis ; b) NCMRWF Coupled Model

4.2 Monsoon 2017

In this section we discuss the simulations of coupled model for all three components: atmosphere, ocean and sea-ice. For atmospheric and ocean models the June-September (JJAS) 2017 is chosen to demonstrate the performance of the coupled model. For sea-ice the peak melting (freezing) season for north (south) pole, July-September (JAS) has been chosen for analysis. The coupled model simulations for different length of time integrations (Day-1 through

9) are compared with the stand-alone atmosphere-land, ocean-sea-ice models respectively. The stand-alone atmosphere model data is taken from NCMRWF medium range forecasts runs from NCUM N768L70 global model real-time outputs (Rakhi et al., 2016). The stand-alone ocean and sea-ice data are taken from NEMO-CICE global model real-time runs made at NCMRWF. The ocean-sea-ice model resolution is 25 km in horizontal and has 75 vertical layers. Though the NCUM atmosphere model at 17 km resolution (N786) is compared to the 65 km resolution (N216) of the coupled model's atmospheric component, we believe it is appropriate to compare large scale features of the monsoon. The Day-1, 5 and 9 forecasts from the coupled model averaged over the season are plotted and compared with analysis and the stand-alone model products. The atmosphere and ocean-sea-ice analysis are taken from their respective data assimilation systems running at NCMRWF in real-time mentioned earlier (Kumar et al., 2018; Momin et al., 2019). The main goal of this exercise is to see if the coupled model is producing the large-scale atmosphere, ocean and sea-ice features realistically in shorter time-scale. This will substantiate the correct implementation of the coupled model configuration and software set-up on Bhaskara HPC.

4.2.1 Atmospheric parameters

Figure 5 shows the comparison of mean monsoon 2017 winds at 850 hPa from both the coupled and stand alone NCUM atmospheric model. Mean JJAS circulation from analysis is also shown. Broadly, low-level monsoon flow features like the cross equatorial flow (CEF), low-level westerly jet (LLJ) and the monsoon trough (MT) are captured by the coupled model and compare well with analysis and NCUM forecasts. Figure 6 show the comparison of winds at 500 hPa. The mean east-west trough seen in the analysis is brought out well by the coupled model. Figure 7 shows the 200 hPa winds from both models and the analysis. The Tibetan anti-cyclone (TAC) and the tropical easterly jet (TEJ) are both captured well in the coupled model. Figure 8 shows the large scale distribution of rainfall during monsoon 2017 over India and adjoining seas. The coupled model is able to capture rainfall over monsoon trough region (central India), Western Ghats, foothills of Himalayas, Arakan coast (Myanmar) and equatorial Indian Ocean.

4.2.2 Ocean parameters

Figure 9 shows the simulated SST from coupled and stand-alone global NEMO model. The broad features are captured well in the Indian Ocean region. Relatively cooler SSTs off the Somali coastal region and south-east of off the Arabian Peninsula are captured well. Warmer

SSTs in the northern Bay of Bengal (BoB) are also captured well. Overall the north-south and east-west SST gradients are also simulated well from Day-1 through Day-9. Figure 10 shows the simulated Sea Surface Salinity (SSS) from both the coupled and stand-alone NEMO model. The contrasting SSSs over Arabian Sea and BoB are brought out well. The very low saline water near head BoB is captured well. Figure 11 shows the simulated surface ocean currents from the coupled and stand alone NEMO model. Major features of Indian Ocean surface circulation like Southern Gyre (SG), Great Whirl (GW), Socotra Eddy (SE), West Indian Coastal Current (WICC), Southwest Monsoon Current (SMC) and equatorial currents are captured well. The semi-permanent eddies in the BoB are also simulated well.

4.2.3 Sea-ice parameters

The sea-ice component of the coupled system comes from the CICE model described earlier. The stand-alone ocean-sea-ice modeling system also has CICE as its sea-ice component. Figure 12 to 15 show the sea-ice fraction and sea-ice drifts for Arctic and Antarctic regions. Sea-ice distribution and associated drifts during Arctic melting season (JAS) are captured well. Similarly for South Pole, the Antarctic sea-ice and associated drifts during freezing season (JAS) are simulated well.

4.2.4 Coupled Model Forecasts: Day 11 and Day 15

The coupled model currently implemented at NCMRWF produce forecasts up to 15 days. This provides extended forecasts compared to standalone atmosphere and ocean models which provide forecast only up to 10 days. In previous section, we discussed the forecasts up to day-9 from both standalone and coupled models. It will be of interest to see how the coupled model performs beyond day-9 and up to day-15. We compare the mean monsoon large-scale features from coupled model with the analysis for the same fields as done in the previous section. Figures 16, 17 and 18 show the day-11 and 15 forecasts from the coupled model along with the analysis fields from atmosphere, ocean and sea-ice components respectively. The coupled model captures the low level monsoon trough, cross equatorial flow and upper level anticyclone reasonably well in day-15 forecast (Figure 16). It can be seen in Figure 17 that the sea surface temperature and surface salinity spatial patterns are represented well up to day-15 forecast. Further, most ocean surface circulations like SG, WICC, SMC and semi-permanent eddies in the BoB are simulated well up to day-15 also. Similarly, the day-15 forecast of sea-ice fraction (Figure 18) and drift velocities compares reasonably with analysis for both north and south Polar regions.

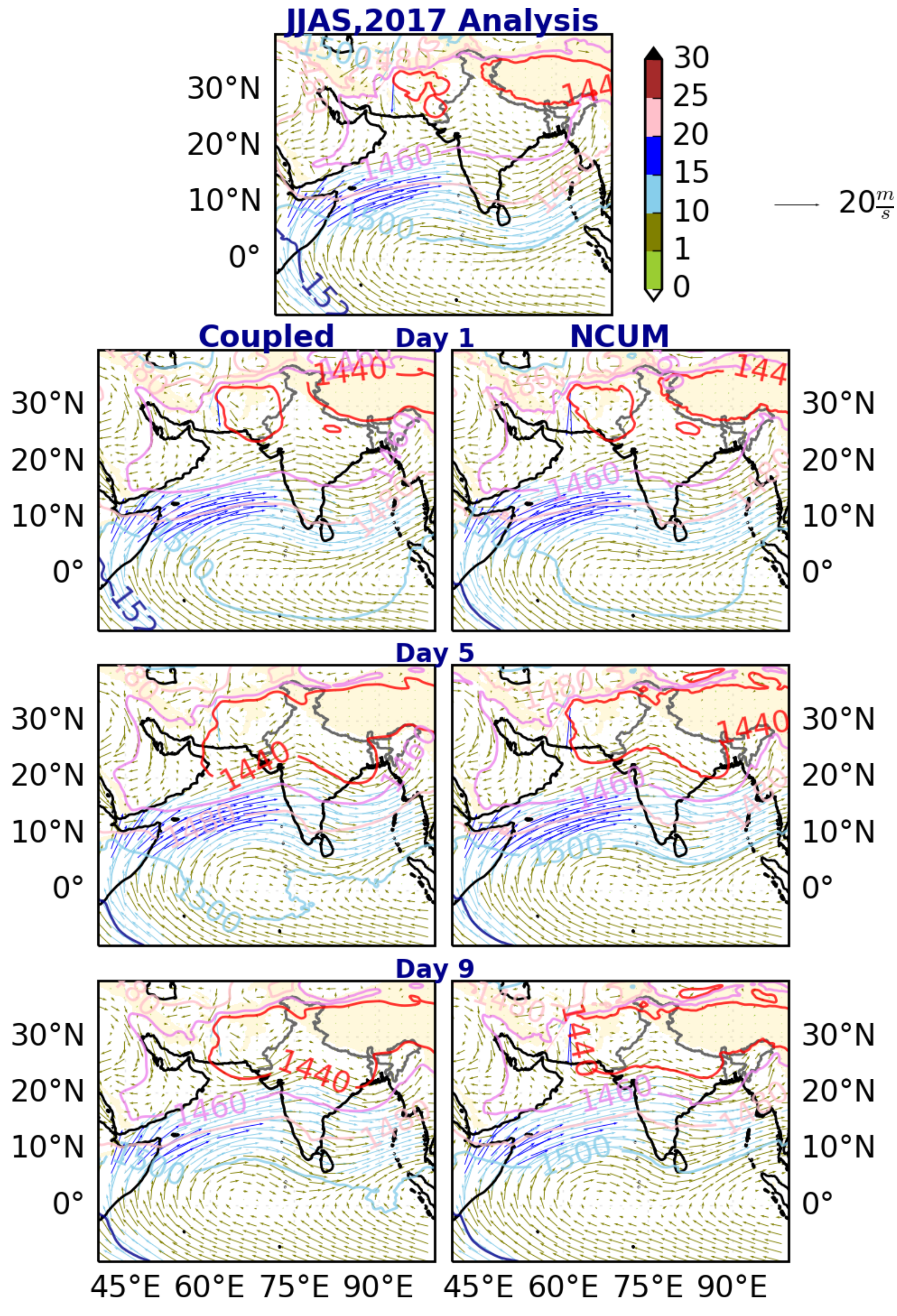

Figure 5: 2017 JJAS mean winds (m/s) and geopotential height (m)(top) analysis and day 1,5,9 forecasts from (left) coupled model and (right) NCUM at 850 hPa

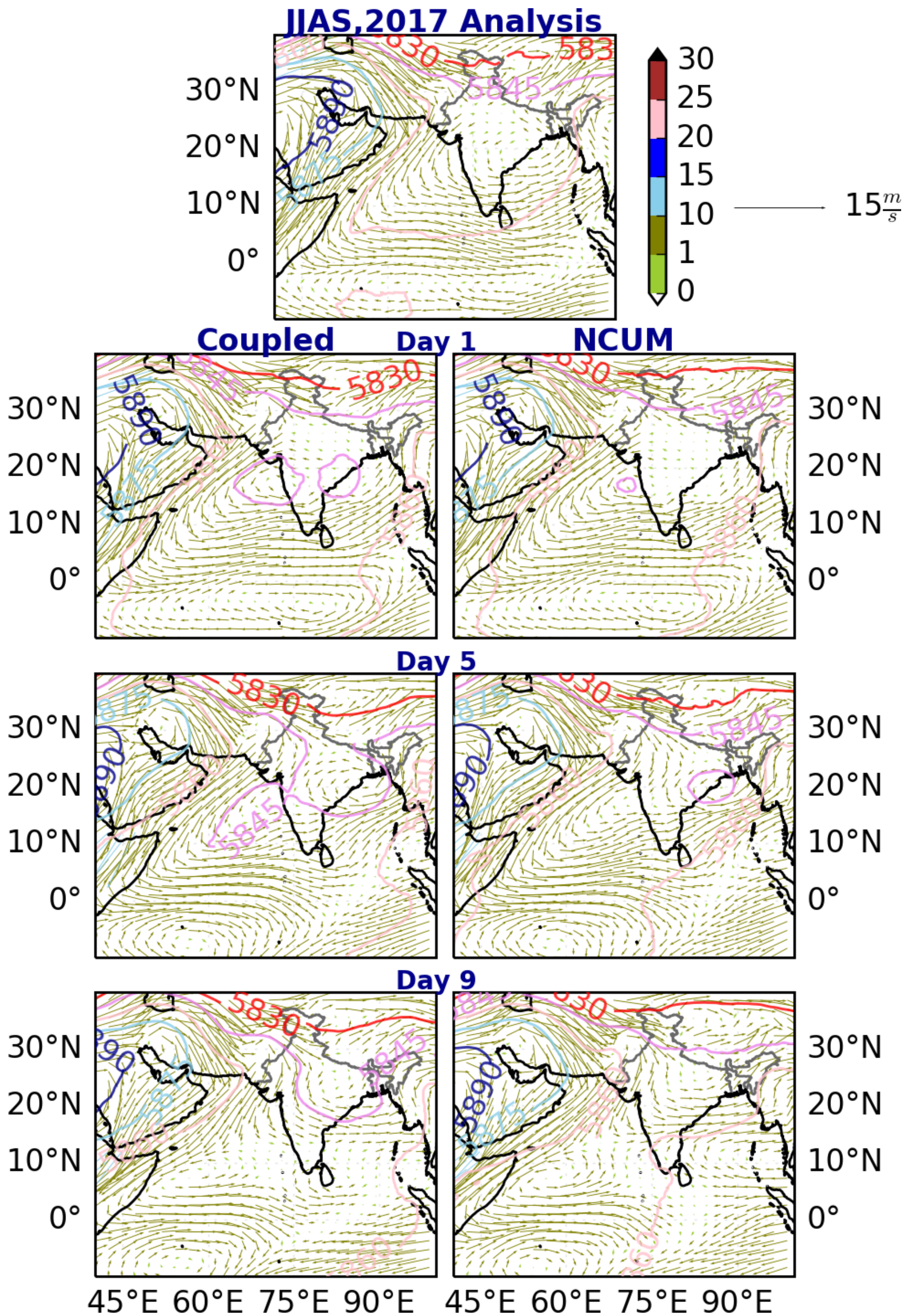

Figure 6: 2017 JJAS mean winds (m/s) and geopotential height (m) (top) analysis and day 1,5,9 forecasts from (left) coupled model and (right) NCUM at 500 hPa

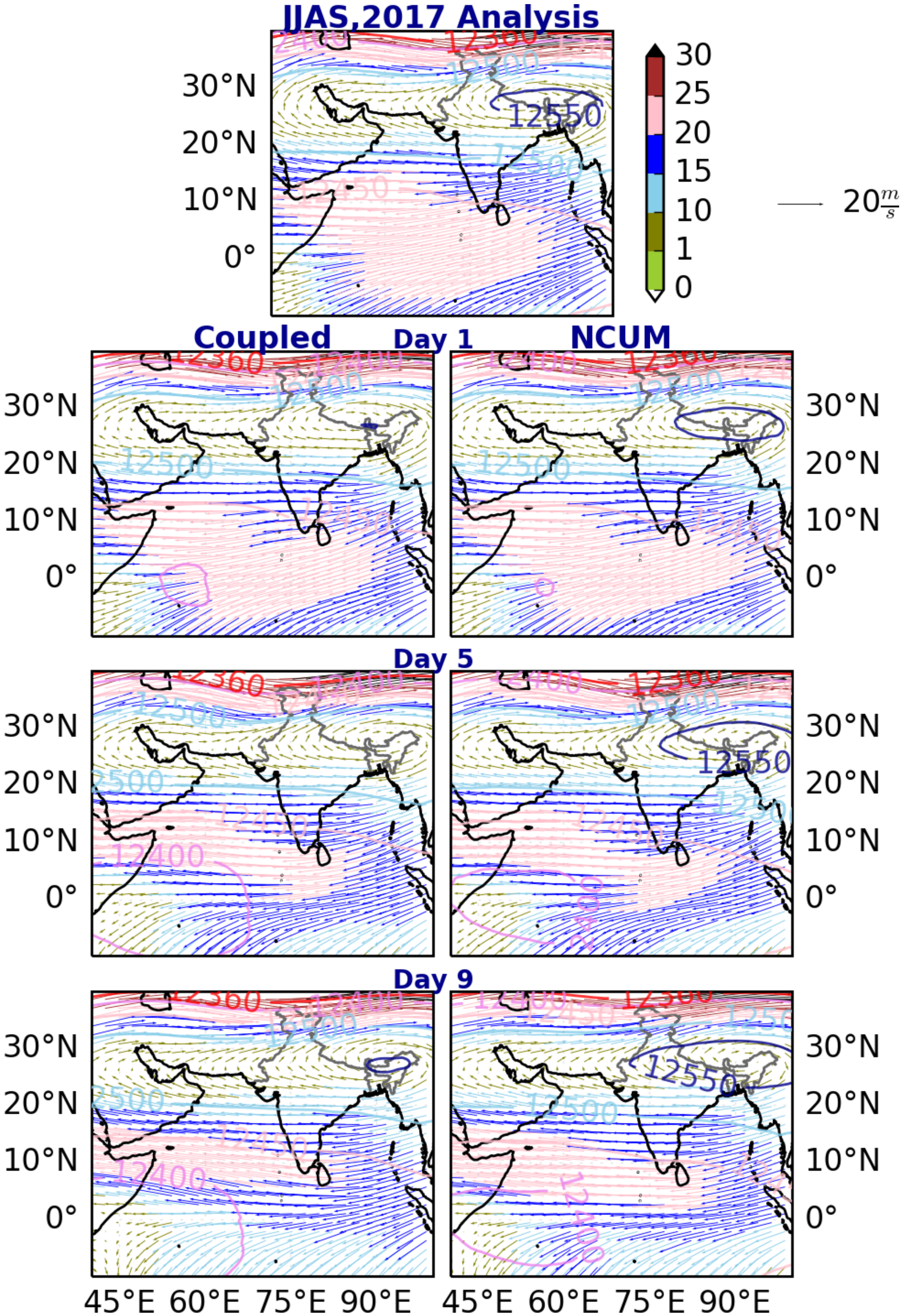

Figure 7: 2017 JJAS mean winds (m/s) and geopotential height (m) (top) analysis and day 1,5,9 forecasts from (left) coupled model and (right) NCUM at 200 hPa

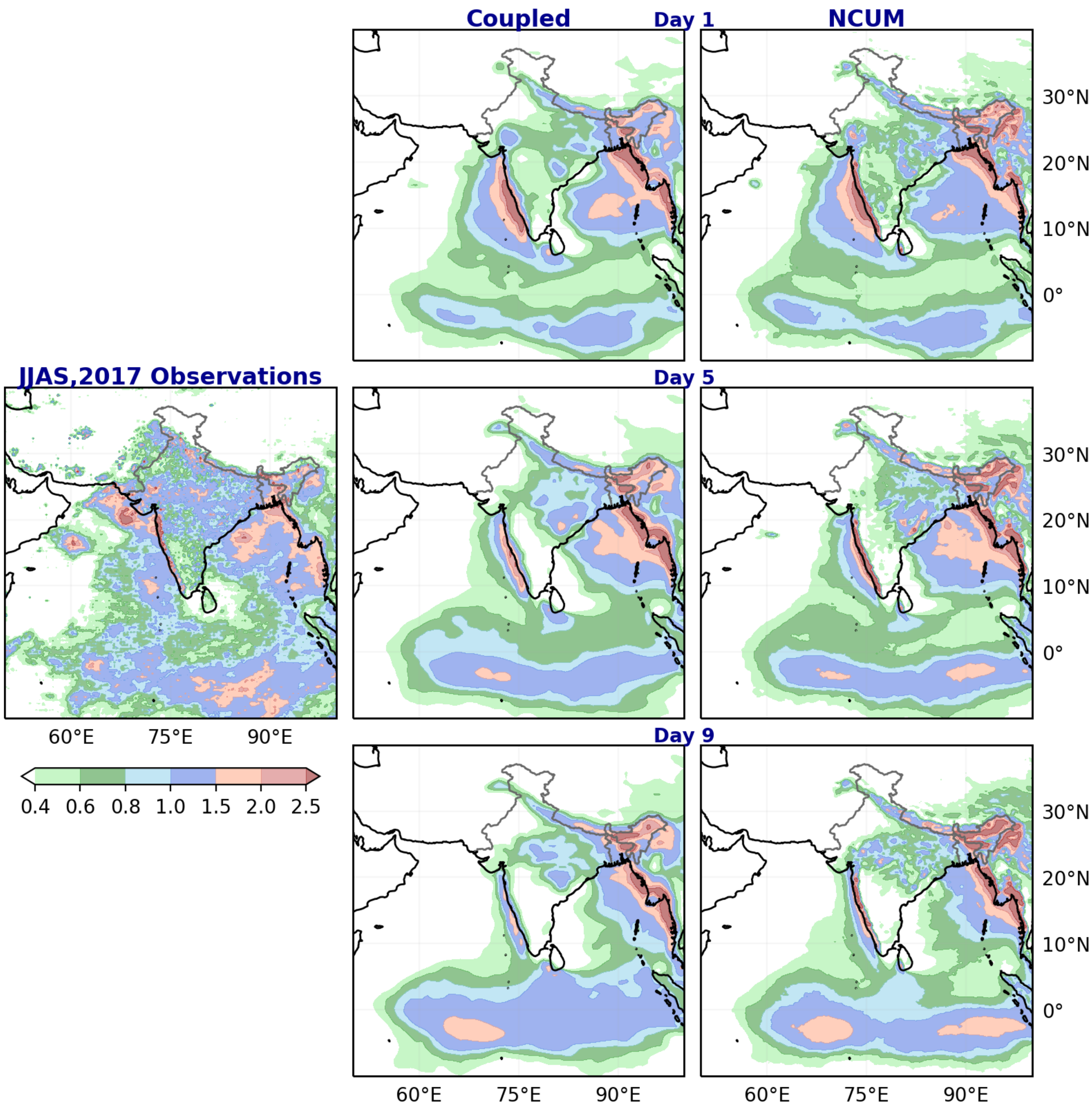

Figure 8: 2017 JJAS mean precipitation (cm/day) (top) observations and day 1,5,9 forecasts from (left) coupled model and (right) NCUM

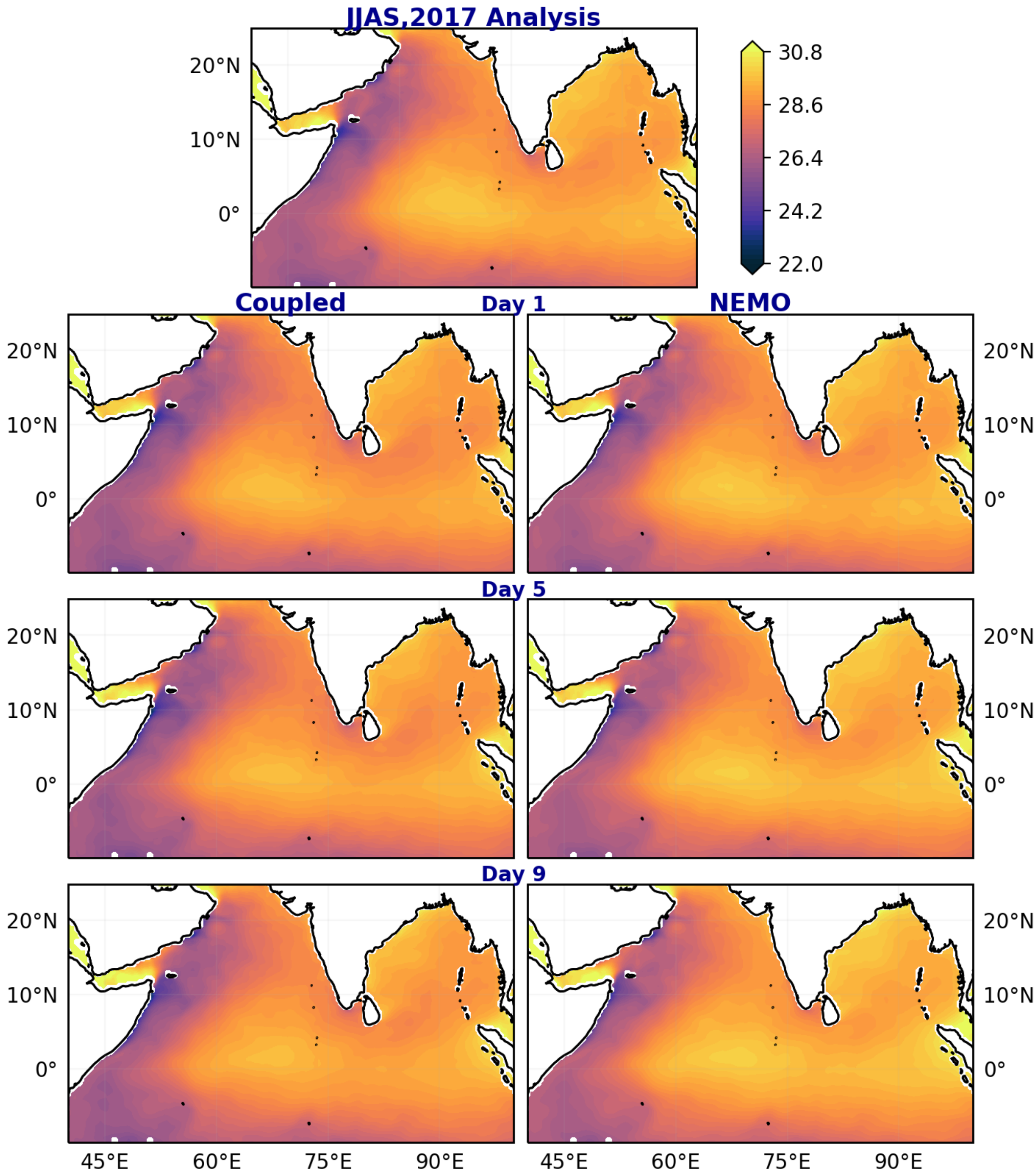

Figure 9: 2017 JJAS mean SST (^{0}C) (top) analysis and day 1,5,9 forecasts from (left) coupled model and (right) NEMO

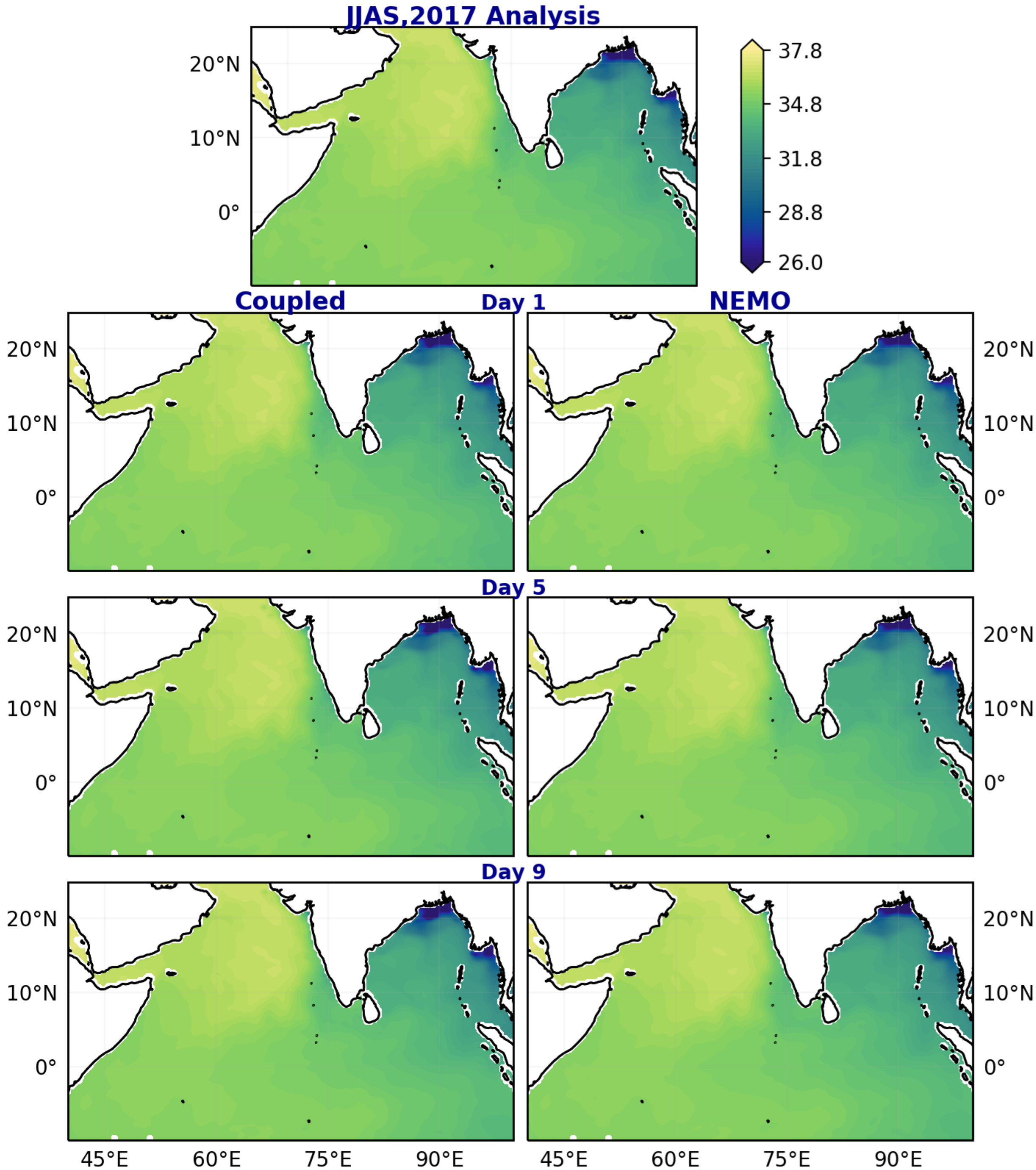

Figure 10: 2017 JJAS mean SSS (psu) (top) analysis and day 1,5,9 forecasts from (left) coupled model and (right) NEMO

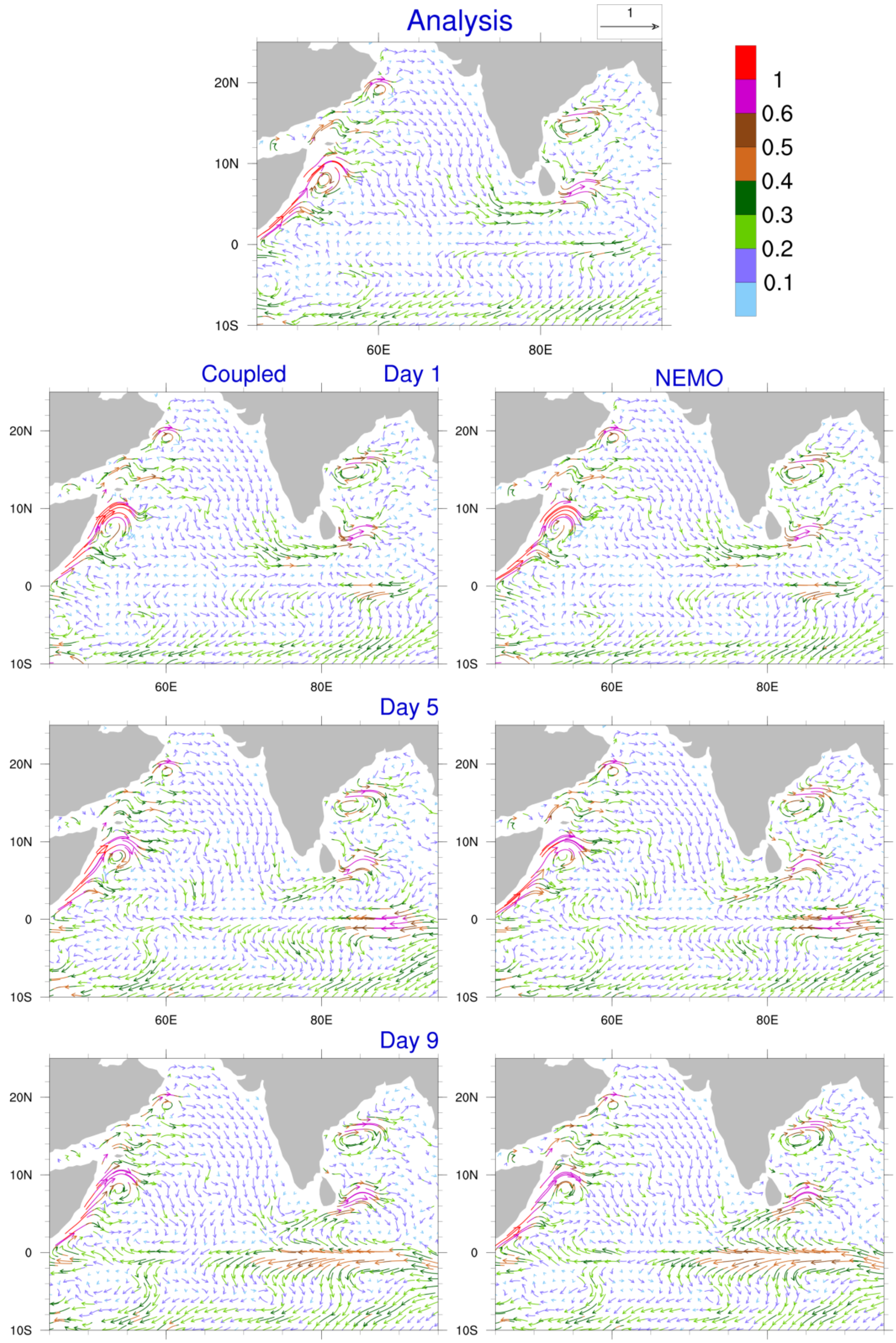

Figure 11: 2017 JJAS mean surface currents (m/s) (top) analysis and day 1,5,9 forecasts from (left) coupled model and (right) NEMO

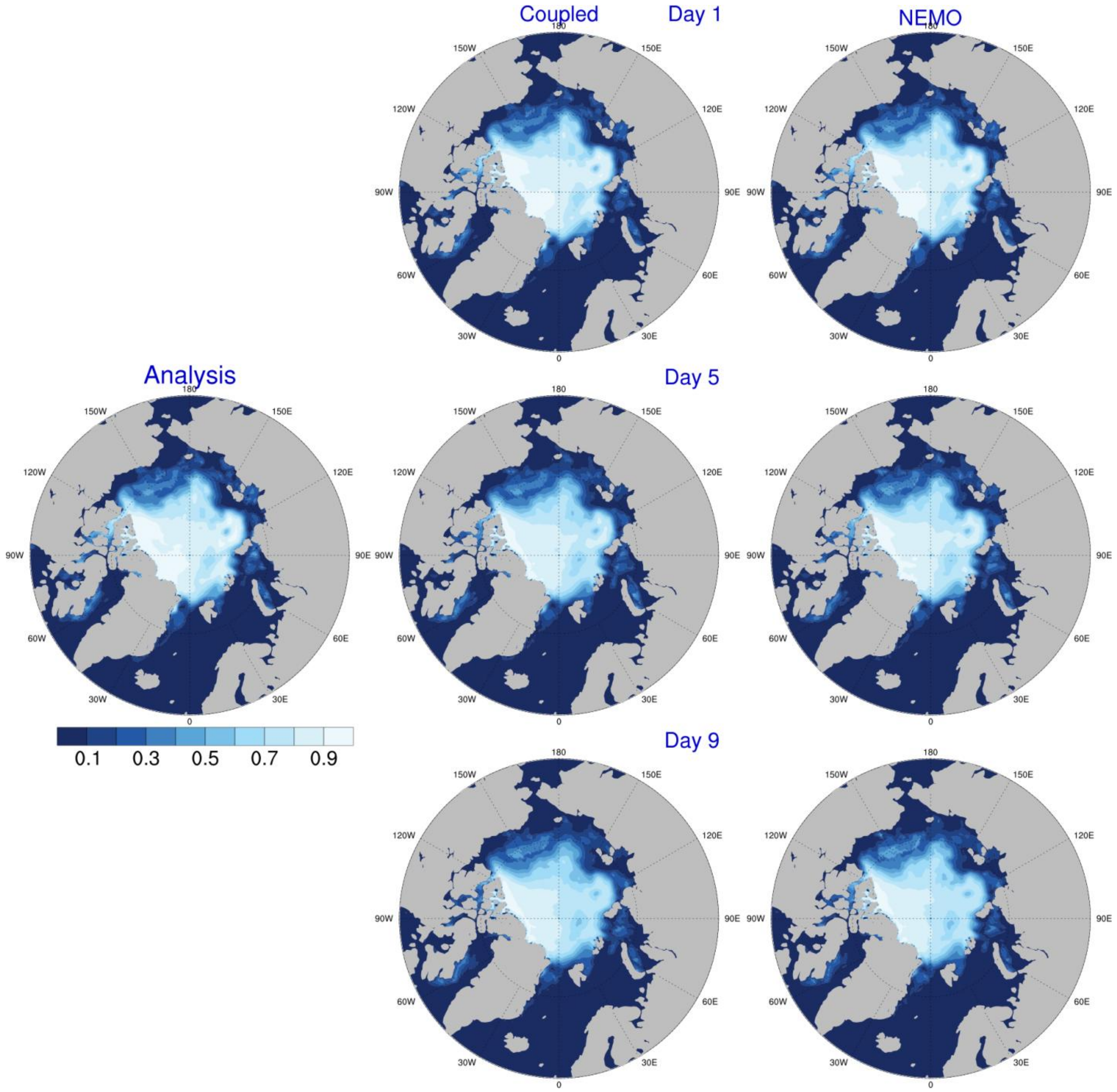

Figure 12: 2017 JAS mean Sea-Ice fraction(-) (top) analysis and day 1,5,9 forecasts from (left) coupled model and (right) NEMO-CICE for northern hemisphere

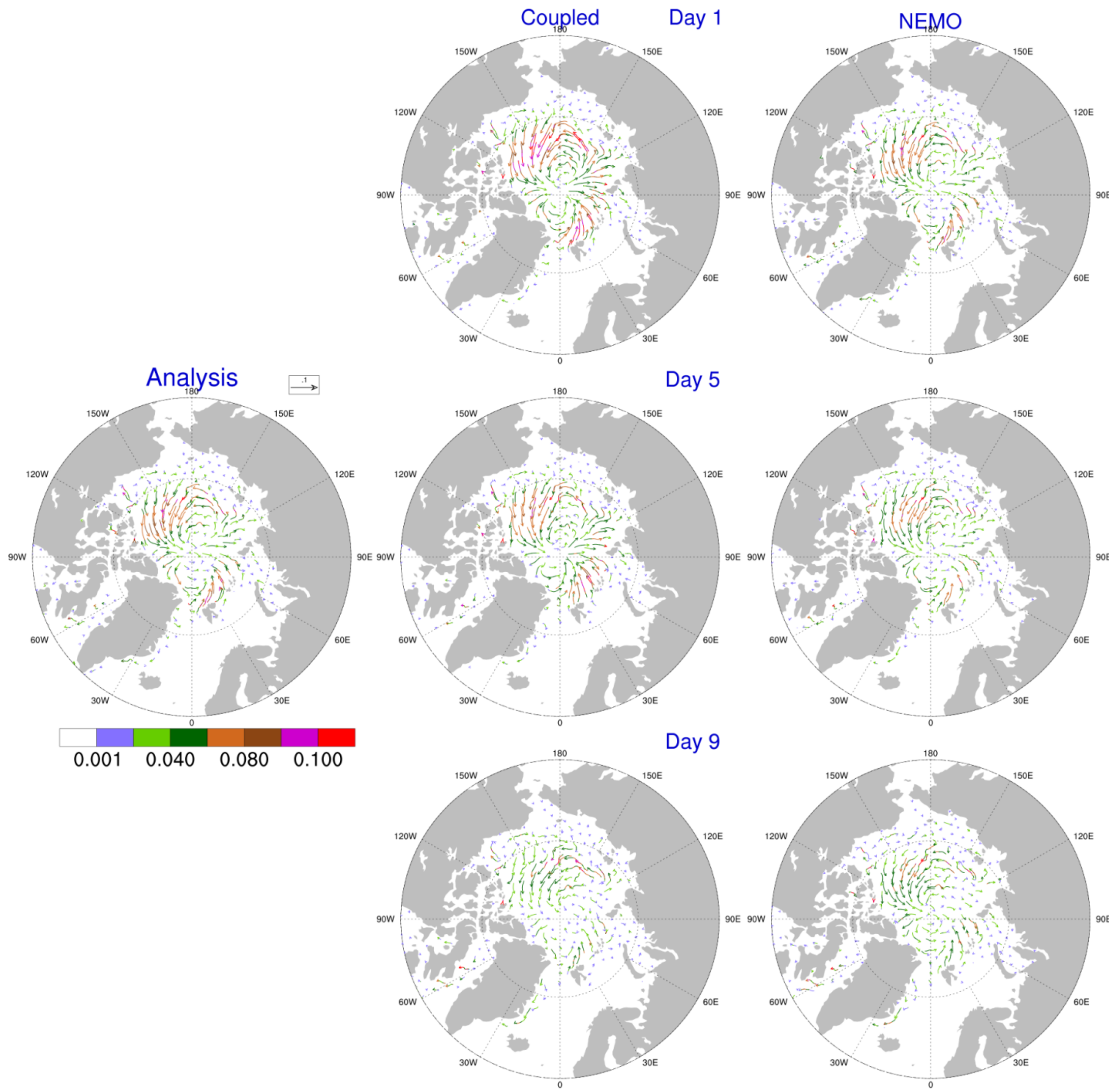

Figure 13: 2017 JAS mean ice-drift (m/s) (top) analysis and day 1,5,9 forecasts from (left) coupled model and (right) NEMO-CICE for northern hemisphere

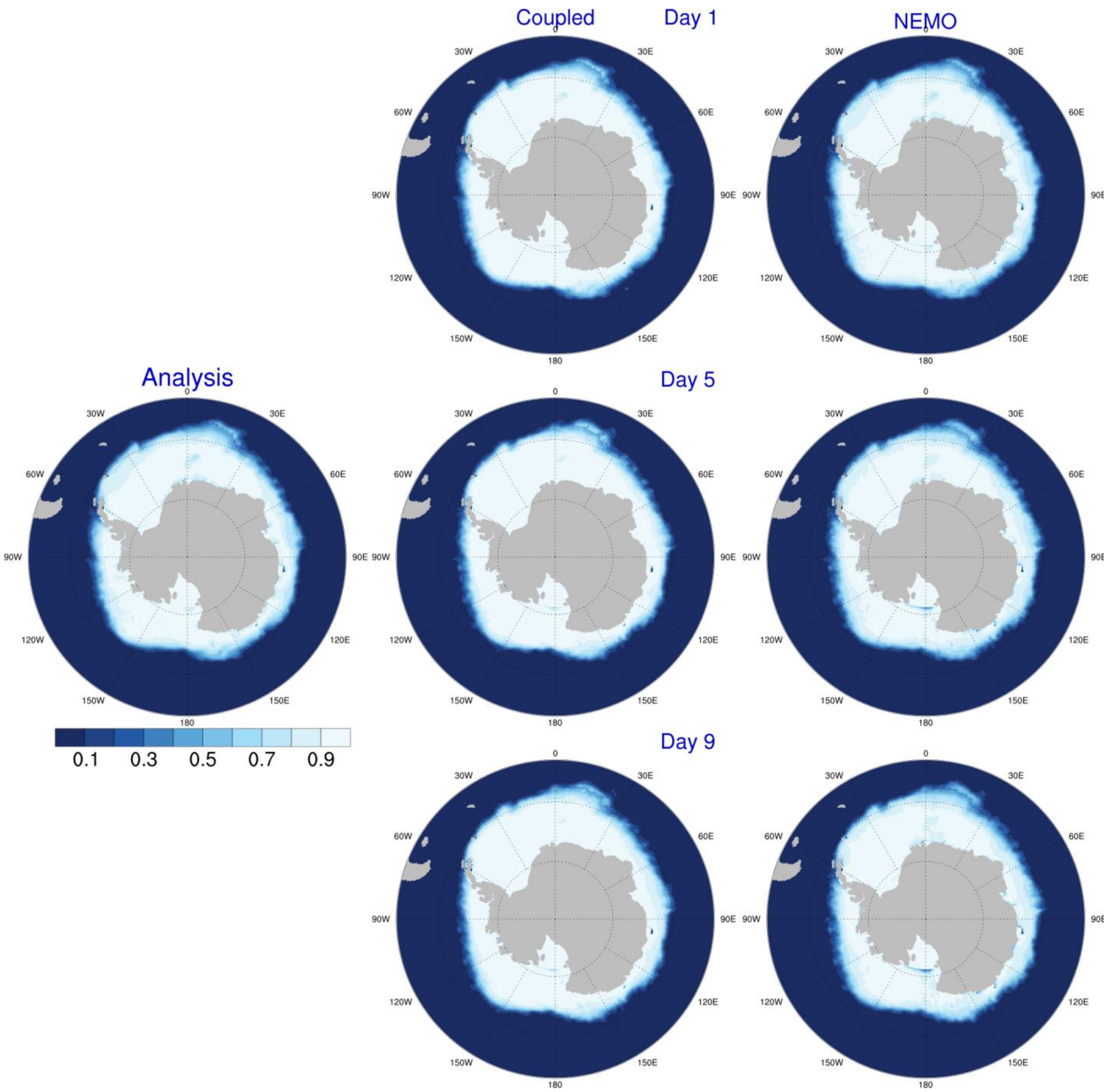

Figure 14: 2017 JAS mean Sea-Ice fraction(-) (top) analysis and day 1,5,9 forecasts from (left) coupled model and (right) NEMO-CICE for southern hemisphere

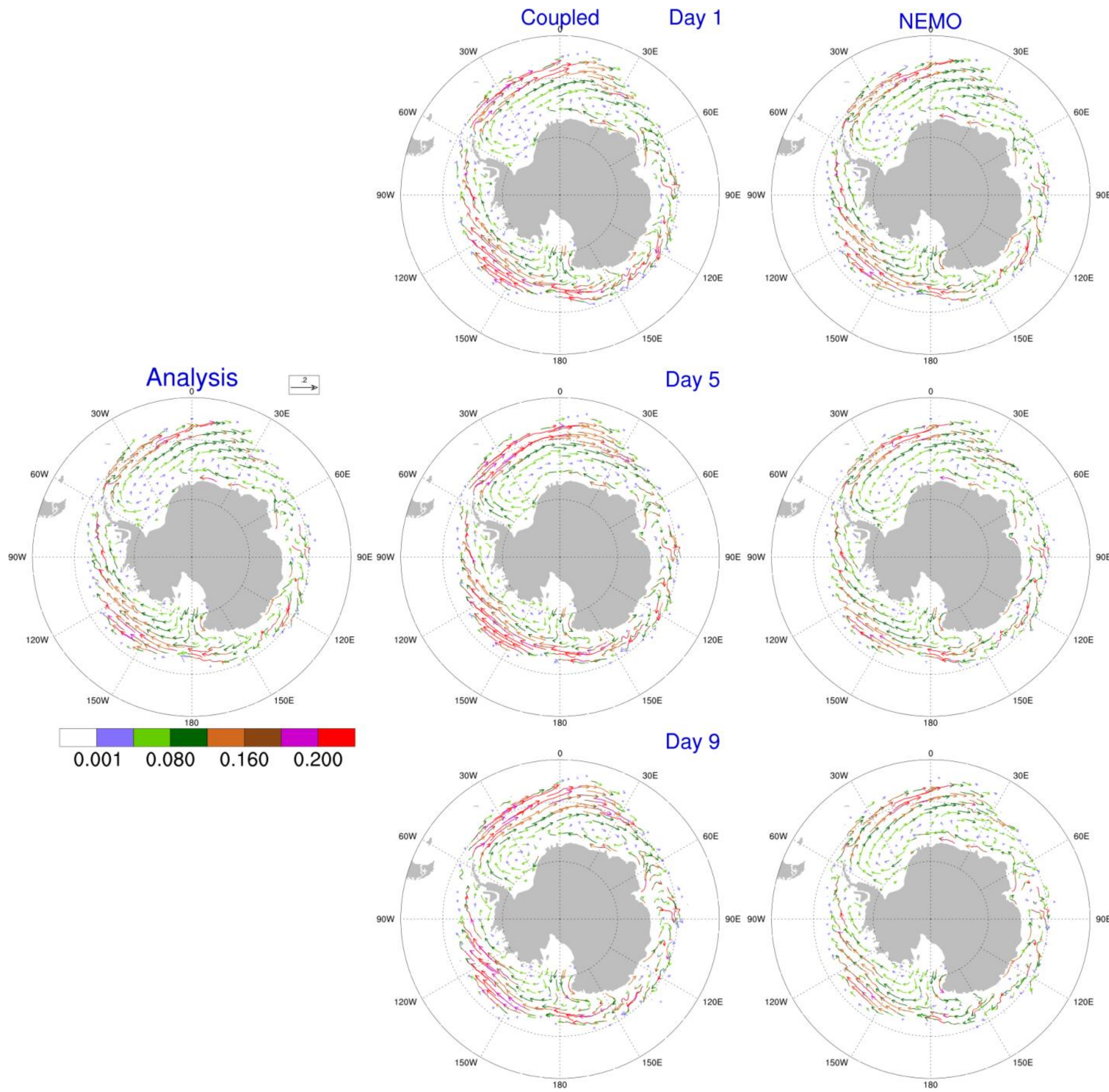

Figure 15: 2017 JAS mean ice-drift (m/s) (top) analysis and day 1,5,9 forecasts from (left) coupled model and (right) NEMO-CICE for southern hemisphere

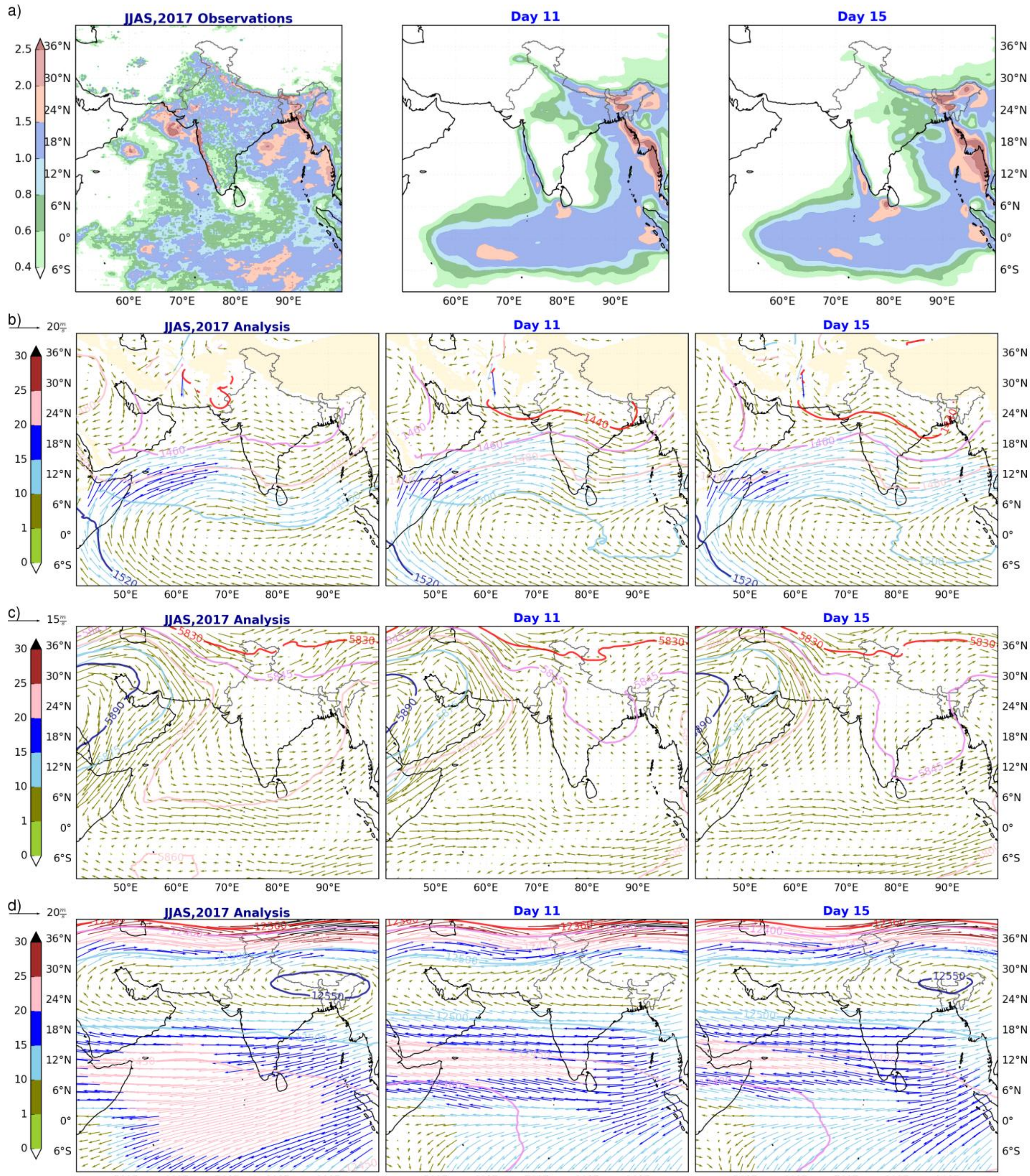

***Figure 16:* 2017 JJAS mean atmospheric variables: analysis (left), and day-11 (center) and day-15 (right) forecasts for a) precipitation and circulation at b) 850 hPa, c) 500 hPa, and d) 200 hPa.**

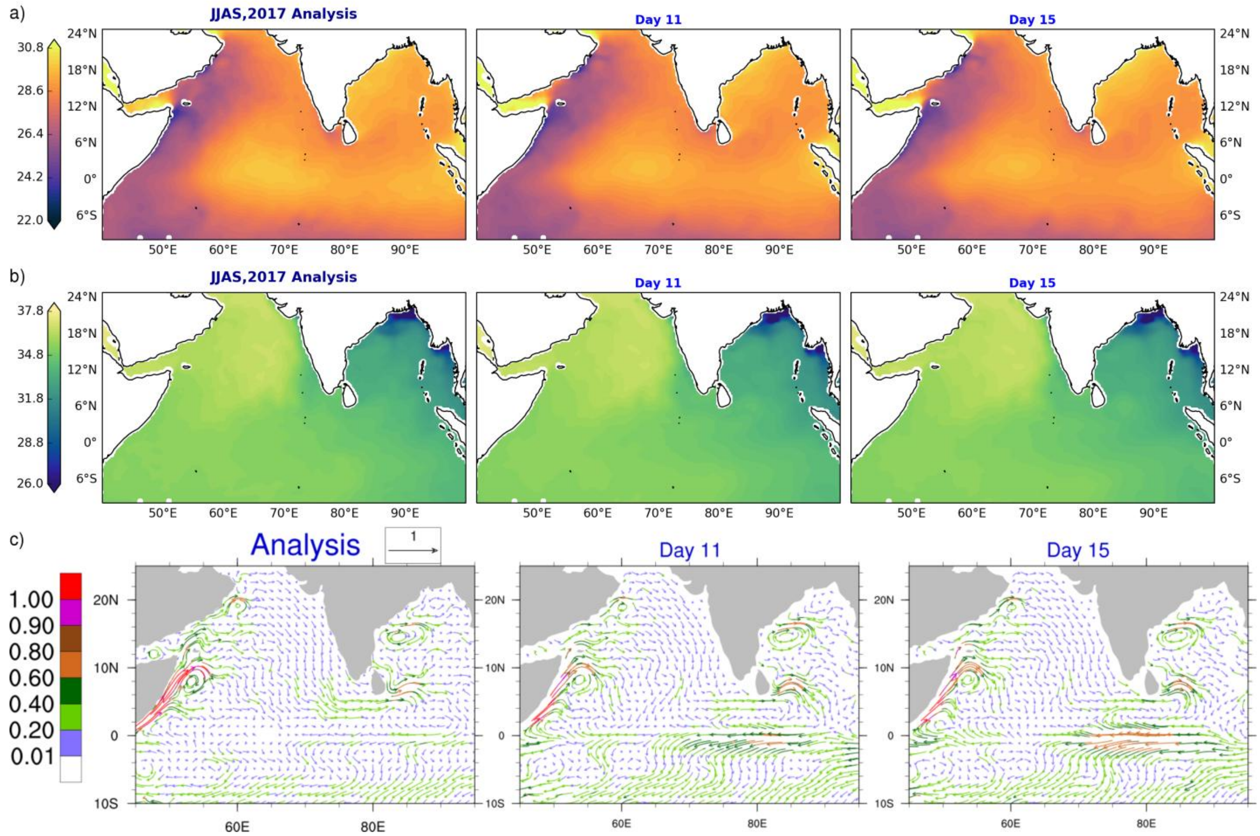

Figure 17: *2017 JJAS mean oceanic variables: analysis (left), and day-11 (center) and day-15 (right) forecasts for a) SST, b) SSS, and c) surface currents*

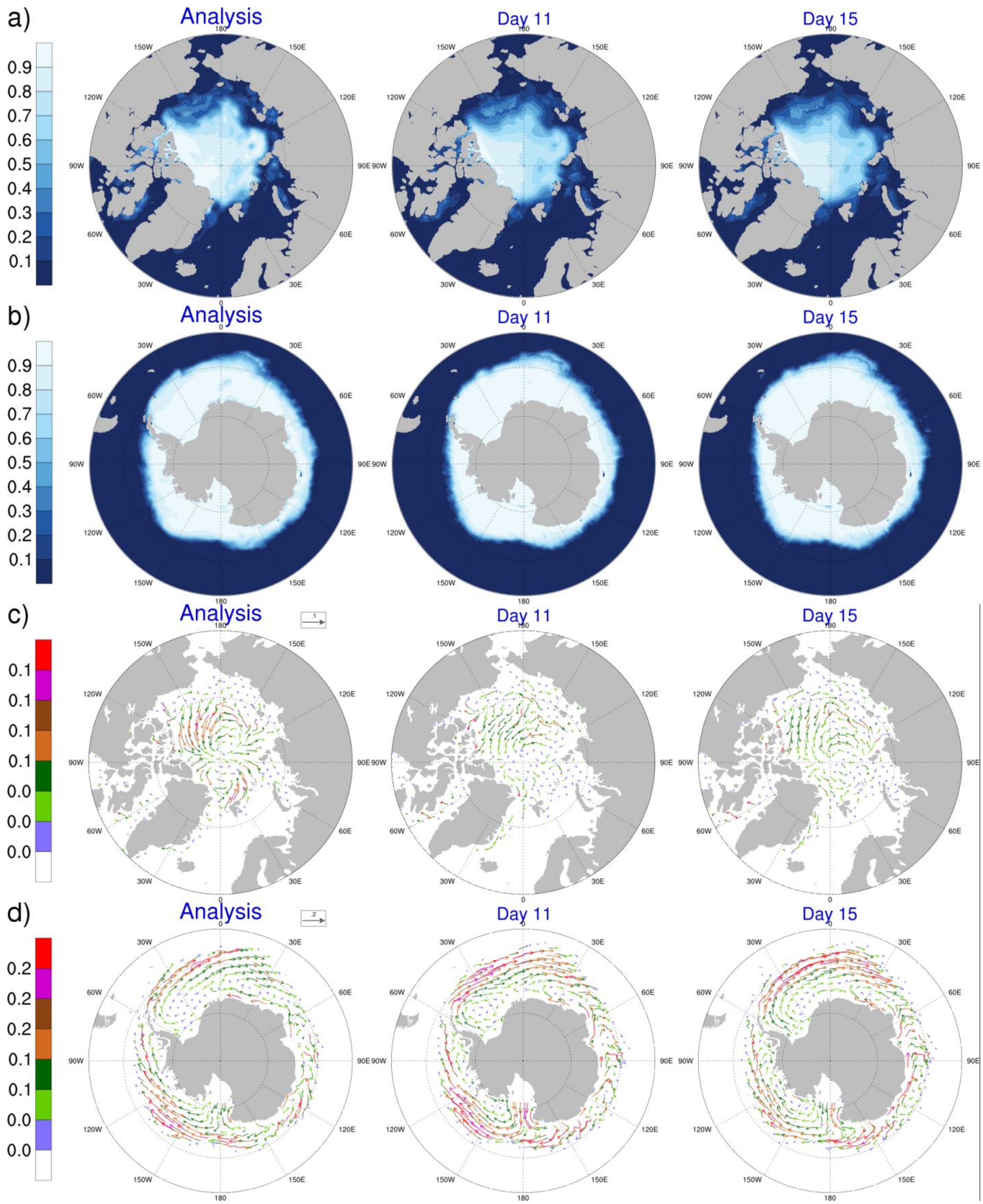

***Figure 18:* 2017 JAS mean sea-ice variables: analysis (left), and day-11 (center) and day-15 (right) forecasts for sea-ice fraction in a) Arctic b) Antarctic region and drift velocities in c) Arctic and d) Antarctic region**

5 Summary

An advanced global coupled ocean-atmosphere-land-seaice model has been implemented at NCMRWF. The current implementation of coupled model is part of the seamless modeling strategy to allow forecast from short to seasonal scales using the same dynamical cores. In this report, details of implementation of the coupled suite at NCMRWF are provided. Brief description of the software used as task manager, scheduler and configuration manager is included. The coupling-specific branches of the Unified Modelling system as well as NEMO and CICE codes are discussed. The interdependency and description of each of the component tasks in operational suite are outlined. The interpolation method, temporal and spatial treatment of coupling-fields, order of interpolation accuracy, and coupling frequency are also all described.

The model is initialized by state-of-art atmospheric, ocean and sea-ice analyses produced in real-time at NCMWRF. The real-time products include weather maps for upto 15-days and plots of simulated and derived ocean, sea-ice parameters. The ocean products provide forecasts of sub-daily and daily variability of the upper ocean. Analysis of tropical cyclones considered, shows that coupled model captures early detection of storms facilitating early warning systems. Further, the location of storm is better captured in coupled model in the case studied here. Coupled model is also able to predict SSTs, TCHP and other ocean parameters in the medium range associated with the cyclone. Analyses of 2017 JJAS (JAS) mean atmospheric and ocean (sea-ice) fields also show that coupled model is able to simulate the large scale features for all components: land-atmosphere, ocean and sea-ice reasonably well. Up to day-9 the coupled model features compare well with stand-alone atmosphere and ocean model simulations at NCMRWF. Beyond day-9 and up to day-15 the coupled model features compare well with the analyses. We plan to configure this GC2 coupled system at various resolutions to implement coupled NWP (medium range), Extended Range (multi-week) and Seasonal time scales, which will be part of NCMRWF Seamless Prediction System.

Acknowledgements

The authors are thankful to Secretary, MoES for his constant encouragement for the coupled model program of NCMRWF. The authors like to acknowledge the Met Office and UM Partnership for providing the coupled suite and related codes. We also like to thanks NEMO EU Consortium and CICE Consortium for providing respectively the ocean and sea-ice model codes.

We are thankful to Joao Teixeira, Livia Thorpe and Sean F. Milton from Met Office for their help and support in the implementation of the coupled model at NCMRWF.

References

Abhilash, S., A. K. Sahai, N. Borah, R. Chattopadhyay, S. Joseph, S. Sharmila, S. De, B. N. Goswami, and Arun Kumar. 2014. "Prediction and Monitoring of Monsoon Intraseasonal Oscillations over Indian Monsoon Region in an Ensemble Prediction System Using CFSv2." *Climate Dynamics*.

Amante, C., and B.W. W. Eakins. 2009. "ETOPO1 – 1 Arc-Minute Global Relief Model: Procedures, Data Sources and Analysis." *NOAA Technical Memorandum NESDIS NGDC-24*.

Beckmann, A, and R Döscher. 1997. "A Method for Improved Representation of Dense Water Spreading over Topography in Geopotential-Coordinate Models." *Journal of Physical Oceanography* 27 (4): 581–91.

Bell, Michael, Michel Lefèbvre, Pierre-Yves Le Traon, Neville Smith, and Kirsten Wilmer-Becker. 2009. "GODAE: The Global Ocean Data Assimilation Experiment." *Oceanography*.

Best, M J, M Pryor, D B Clark, G G Rooney, R Essery, C B Ménard, J M Edwards, et al. 2011. "The Joint UK Land Environment Simulator (JULES), Model Description--Part 1: Energy and Water Fluxes." *Geoscientific Model Development* 4 (3): 677–99.

Bitz, Cecilia M, and William H Lipscomb. 1999. "An Energy-Conserving Thermodynamic Model of Sea Ice." *Journal of Geophysical Research: Oceans* 104 (C7): 15669–77.

Charney, Jg G, and J Shukla. 1981. "Predictability of Monsoons." In *Monsoon Dynamics*.

Demott, Charlotte A, Nicholas P Klingaman, and Steven J Woolnough. 2015. "Reviews of Geophysics Atmosphere-Ocean Coupled Processes in the Madden-Julian Oscillation."

Edwards, J M, and A Slingo. 1996. "Studies with a Flexible New Radiation Code. I: Choosing a Configuration for a Large-Scale Model." *Quarterly Journal of the Royal Meteorological Society* 122 (531): 689–719.

Gaspar, Philippe, Yves Grégoris, and Jean-Michel Lefevre. 1990. "A Simple Eddy Kinetic Energy Model for Simulations of the Oceanic Vertical Mixing: Tests at Station Papa and Long-Term Upper Ocean Study Site." *Journal of Geophysical Research: Oceans* 95 (C9): 16179–93.

George, J P, S Indira Rani, A Jayakumar, S Mohandas, S Mallick, A Lodh, R Rakhi, M N R Sreevathsa, and E N Rajagopal. 2016. "NCUM Data Assimilation System."

Gregory, D, and P R Rowntree. 1990. "A Mass Flux Convection Scheme with Representation of Cloud Ensemble Characteristics and Stability-Dependent Closure." *Monthly Weather Review* 118 (7): 1483–1506.

Hunke, E C, and J K Dukowicz. 1997. "An Elastic--Viscous--Plastic Model for Sea Ice Dynamics." *Journal of Physical Oceanography* 27 (9): 1849–67.

IOC, I H O, and BODC In. 2003. "Centenary Edition of the GEBCO Digital Atlas, Published on CD-ROM on Behalf of the Intergovernmental Oceanographic Commission and the International Hydrographic Organization as Part of the General Bathymetric Chart of the Oceans." *British Oceanographic Data Centre*.

Kumar, Sumit, S Indira Rani, John P George, and E N Rajagopal. 2018. "Megha-Tropiques SAPHIR Radiances in a Hybrid 4D-Var Data Assimilation System: Study of Forecast

Impact." *Quarterly Journal of the Royal Meteorological Society* 144 (712): 792–805.
Lock, A P, A R Brown, M R Bush, G M Martin, and R N B Smith. 2000. "A New Boundary Layer Mixing Scheme. Part I: Scheme Description and Single-Column Model Tests." *Monthly Weather Review* 128 (9): 3187–99.
Lott, François, and Martin J Miller. 1997. "A New Subgrid-Scale Orographic Drag Parametrization: Its Formulation and Testing." *Quarterly Journal of the Royal Meteorological Society* 123 (537): 101–27.
Maclachlan, C., A. Arribas, K. A. Peterson, A. Maidens, D. Fereday, A. A. Scaife, M. Gordon, et al. 2015. "Global Seasonal Forecast System Version 5 (GloSea5): A High-Resolution Seasonal Forecast System." *Quarterly Journal of the Royal Meteorological Society* 141 (689): 1072–84.
Martin, G. M., N. Bellouin, W. J. Collins, I. D. Culverwell, P. R. Halloran, S. C. Hardiman, T. J. Hinton, et al. 2011. "The HadGEM2 Family of Met Office Unified Model Climate Configurations." *Geoscientific Model Development* 4 (3): 723–57.
Megann, A., D. Storkey, Y. Aksenov, S. Alderson, D. Calvert, T. Graham, P. Hyder, J. Siddorn, and B. Sinha. 2014. "GO5.0: The Joint NERC-Met Office NEMO Global Ocean Model for Use in Coupled and Forced Applications." *Geoscientific Model Development* 7 (3): 1069–92.
Mesinger, Fedor, and Akio Arakawa. 1976. "Numerical Methods Used in Atmospheric Models."
Mitra, Ashis K., E. N. Rajagopal, G. R. Iyengar, D. K. Mahapatra, I. M. Momin, A. Gera, K. Sharma, J. P. George, R. Ashrit, M. Dasgupta, S. Mohandas, V. S. Prasad, S. Basu, A. Arribas, S. F. Milton, G. M. Martin, D. Barker, M. Martin. 2013. "Prediction of Monsoon Using a Seamless Coupled Modelling System." *Current Science*: 1369-1379
Momin, Imranali M, Ashis Kumar Mitra, J Waters, M J Martin, and Rajagopal E N. 2019. "Impact of Altika Sea Level Anomaly Data on a Variational Assimilation System." *Journal of Coastal Research*.(Under Review)
Rae, J. G L, H. T. Hewitt, A. B. Keen, J. K. Ridley, A. E. West, C. M. Harris, E. C. Hunke, and D. N. Walters. 2015. "Development of the Global Sea Ice 6.0 CICE Configuration for the Met Office Global Coupled Model." *Geoscientific Model Development* 8 (7): 2221–30.
Rakhi, R, A Jayakumar, M N R Sreevathsa, and E N Rajagopal. 2016. "Implementation and Up-Gradation of NCUM in Bhaskara HPC."
Sarkar, Sahadat, Parthasarathi Mukhopadhyay, Ravuri Phani Murali Krishna, and Somenath Dutta. 2018. "Coupled Model Fidelity in Capturing Atmospheric Internal Processes during Organization and Intensification of Boreal Summer Intra-Seasonal Oscillation." *International Journal of Climatology* 38 (14): 5339–53.
Scaife, A A, N Butchart, C D Warner, and R Swinbank. 2002. "Impact of a Spectral Gravity Wave Parameterization on the Stratosphere in the Met Office Unified Model." *Journal of the Atmospheric Sciences* 59 (9): 1473–89.
Simmons, Harper L, Steven R Jayne, Louis C St Laurent, and Andrew J Weaver. 2004. "Tidally Driven Mixing in a Numerical Model of the Ocean General Circulation." *Ocean Modelling* 6 (3–4): 245–63.
Smith, R N B. 1990. "A Scheme for Predicting Layer Clouds and Their Water Content in a General Circulation Model." *Quarterly Journal of the Royal Meteorological Society* 116 (492): 435–60.
Vitart, Frédéric, Robert Buizza, Magdalena Alonso Balmaseda, Gianpaolo Balsamo, Jean Raymond Bidlot, Axel Bonet, Manuel Fuentes, Alfred Hofstadler, Franco Molteni, and Tim

N. Palmer. 2008. “The New VarEPS-Monthly Forecasting System: A First Step towards Seamless Prediction.” *Quarterly Journal of the Royal Meteorological Society*.

Walters, David, Ian Boutle, Malcolm Brooks, Thomas Melvin, Rachel Stratton, Simon Vosper, Helen Wells, et al. 2017. “The Met Office Unified Model Global Atmosphere 6.0/6.1 and JULES Global Land 6.0/6.1 Configurations.” *Geoscientific Model Development* 10 (4): 1487–1520.

Waters, Jennifer, Daniel J Lea, Matthew J Martin, Isabelle Mirouze, Anthony Weaver, and James While. 2015. “Implementing a Variational Data Assimilation System in an Operational 1/4 Degree Global Ocean Model.” *Quarterly Journal of the Royal Meteorological Society* 141 (687): 333–49.

Williams, K. D., C. M. Harris, A. Bodas-Salcedo, J. Camp, R. E. Comer, D. Copsey, D. Fereday, et al. 2015. “The Met Office Global Coupled Model 2.0 (GC2) Configuration.” *Geoscientific Model Development* 8 (5): 1509–24.

Wilson, Damian R, and Susan P Ballard. 1999. “A Microphysically Based Precipitation Scheme for the UK Meteorological Office Unified Model.” *Quarterly Journal of the Royal Meteorological Society* 125 (557): 1607–36.

Wilson, Damian R, Andrew C Bushell, Amanda M Kerr-Munslow, Jeremy D Price, and Cyril J Morcrette. 2008. “PC2: A Prognostic Cloud Fraction and Condensation Scheme. I: Scheme Description.” *Quarterly Journal of the Royal Meteorological Society: A Journal of the Atmospheric Sciences, Applied Meteorology and Physical Oceanography* 134 (637): 2093–2107.

Wood, Nigel, Andrew Staniforth, Andy White, Thomas Allen, Michail Diamantakis, Markus Gross, Thomas Melvin, et al. 2014. “An Inherently Mass-Conserving Semi-Implicit Semi-Lagrangian Discretization of the Deep-Atmosphere Global Non-Hydrostatic Equations.” *Quarterly Journal of the Royal Meteorological Society*.

Appendix A: List of ancillary fields

The fields not read from atmospheric dump are either read from ancillary files or initialized to default values. This appendix provides list of all the ancillary files used during the reconfiguration of the atmospheric dump to provide initial state of the atmosphere.

Table A. 1: Fields read from ancillary files

/gpfs1/home/moum/UM/ancil/atmos/n216e/orca025/iceberg_calving/gc1p0_anbag/v2/qrclim.icecalve
00190: Iceberg Calving Field: Cpl   kg/M2/S
/gpfs1/home/moum/UM/ancil/atmos/n216e/orca025/land_sea_mask/etop01/v1/qrparm.mask
00030: Land Mask (No Halo) (Land=True)
/gpfs1/home/moum/UM/ancil/atmos/n216e/orca025/land_sea_mask/etop01/v1/qrparm.landfrac
00505: Land Fraction In Grid Box
/gpfs1/home/moum/UM/ancil/atmos/n216e/orca025/general_land/GlobAlbedo/v2/qrclim.land
00243: Obs/Clim Snow-Free Surf Sw Albedo
/gpfs1/home/moum/UM/ancil/atmos/n216e/orca025/orography/globe30/v5/qrparm.orog
00005: Orographic Gradient X Component
00006: Orographic Gradient Y Component
00017: Silhouette Orographic Roughness
00018: Half Of (Peak To Trough Ht Of Orog)
00033: Orography (/Strat Lower Bc)
00034: Standard Deviation Of Orography
00035: Orographic Gradient Xx Component
00036: Orographic Gradient Xy Component
00037: Orographic Gradient Yy Component
/gpfs1/home/moum/UM/ancil/atmos/n216e/orca025/soil_parameters/hwsd_vg/v3/qrparm.soil
00040: VolSmc At Wilting After Timestep
00041: VolSmc At Crit Pt After Timestep
00043: VolSmc At Saturation After Timestep
00044: Sat Soil Conductivity After Timestep
00046: Thermal Capacity After Timestep
00047: Thermal Conductivity After Timestep
00048: Saturated Soil Water Suction
00207: Clapp-Hornberger "B" Coefficient
00220: Snow-Free Albedo Of Soil
00223: Soil Carbon Content   kg C / M2
/gpfs1/home/moum/UM/ancil/atmos/n216e/orca025/vegetation/fractions_igbp/v3/qrparm.veg.frac
00216: Fractions Of Surface Types
/gpfs1/home/moum/UM/ancil/atmos/n216e/orca025/vegetation/func_type_modis/v3/qrparm

.veg.func
00217: Leaf Area Index Of Plant Func Types
00218: Canopy Height Of Plant Func Types M
/gpfs1/home/moum/UM/ancil/atmos/n216e/orca025/rivers_trip/sequence/etopo5/v2/qrparm.rivseq
00151: River Sequence
00152: River Direction
/gpfs1/home/moum/UM/ancil/atmos/n216e/orca025/rivers_trip/storage/fekete/v2/qrclim.rivstor
00153: River Water Storage M2
/gpfs1/home/moum/UM/ancil/atmos/n216e/orca025/hydrol_lsh/hydro1k/v1/qrparm.hydtopmn
00274: Mean Topographic Index
/gpfs1/home/moum/UM/ancil/atmos/n216e/orca025/hydrol_lsh/hydro1k/v1/qrparm.hydtopsd
00275: Standard Devn In Topographic Index
/gpfs1/home/moum/UM/ancil/atmos/n216e/aerosol_clims/biom/v4/qrclim.biom85
00352: Clim Biomass-Burning (Fresh) Mmr
00353: Clim Biomass-Burning (Aged) Mmr
00354: Clim Biomass-Burning (In-Cloud) Mmr
/gpfs1/home/moum/UM/ancil/atmos/n216e/aerosol_clims/ocff/v4/qrclim.ocff85
00368: Clim Org C Fossil Fuel (Fresh) Mmr
00369: Clim Org C Fossil Fuel (Aged) Mmr
00370: Clim Org C Fossil Fuel (In-Cloud)Mmr
/gpfs1/home/moum/UM/ancil/atmos/n216e/aerosol_clims/biogenic/v4/qrclim.biog85
00351: Clim Biogenic Aerosol Mmr
/gpfs1/home/moum/UM/ancil/atmos/n216e/aerosol_clims/sslt/v4/qrclim.sslt85
00357: Clim Sea Salt (Film Mode) Npm3
00358: Clim Sea Salt (Jet Mode) Npm3
/gpfs1/home/moum/UM/ancil/atmos/n216e/aerosol_clims/sulp/v4/qrclim.sulp85
00359: ClimSulphate (Accumulation Mode)Mmr
00360: ClimSulphate (Aitken Mode) Mmr
00361: ClimSulphate (Dissolved) Mmr
/gpfs1/home/moum/UM/ancil/atmos/n216e/aerosol_clims/dust/v4/qrclim.dust85
00362: Clim Dust Size Division 1 Mmr
00363: Clim Dust Size Division 2 Mmr
00364: Clim Dust Size Division 3 Mmr
00365: Clim Dust Size Division 4 Mmr
00366: Clim Dust Size Division 5 Mmr
00367: Clim Dust Size Division 6 Mmr
/gpfs1/home/moum/UM/ancil/atmos/n216e/aerosol_clims/blck/v4/qrclim.blck85
00355: Clim Black Carbon (Fresh) Mmr
00356: Clim Black Carbon (Aged) Mmr
/gpfs1/home/moum/UM/ancil/atmos/n216e/ozone/sparc/1994-2005/v2/qrclim.ozone_L85_O85

00060: Ozone

Table A. 2: Fields initialized to zero

00155: Accumulated Surface Runoff kg/M2
00156: Accumulated Sub-Surface Runoff kg/M2
00157: Gridbox Areas M2
00171: Net DnSw Rad Flux:Open Sea: Cpl
00172: Net DwnSfcSw Flux Blw 690Nm: Cpl
00173: Net Down Surface Lw Rad Flux: Cpl
00174: Net DnLw Rad Flux:Open Sea: Cpl
00176: X-Comp Surf &Bl Wind Str: Cpl N/M2
00177: Y-Comp Surf &Bl Wind StrlCpl N/M2
00178: Wind Mix En'GyFl To Sea: Cpl W/M2
00179: SfcShFlx From Open Sea: Cpl W/M2
00180: Sublim. Surface (Gbm): Cpl kg/M2/S
00181: Evap From Open Sea: Cpl kg/M2/S
00184: Heat Flx Through Sea Ice (W/M2): Cpl
00185: Heat Flx In Sea Ice Surface Mlt: Cpl
00186: Large Scale Rain Rate: Cpl kg/M2/S
00187: Large Scale Snow Rate: Cpl kg/M2/S
00188: Convective Rain Rate: Cpl kg/M2/S
00189: Convective Snow Rate: Cpl kg/M2/S
00191: 10 Metre Wind Speed On C Grid: Cpl
00192: River Runoff: Cpl
00222: Net Energy Change This Period J/M**2
00235: Net Moisture Flux In Period kg/M**2
00290: Daily Accumulated Lake Flux kg/M2
00511: InlandbasinflowAtm Grid kg/M2/S

Appendix B: List of simulated variables

Table B. 1: List of simulated variables for atmospheric model

Fields in file cplhca_pa000

Sl No.	STASH Code	Field Name	Frequency
1	31	FRAC OF SEA ICE IN SEA AFTER TSTEP	6 Hrly
2	33	OROGRAPHY (/STRAT LOWER BC)	6 Hrly
3	3225	10 METRE WIND U-COMP B GRID	6 Hrly
4	3226	10 METRE WIND V-COMP B GRID	6 Hrly
5	3236	TEMPERATURE AT 1.5M	6 Hrly
6	3245	RELATIVE HUMIDITY AT 1.5M	6 Hrly
7	3247	VISIBILITY AT 1.5M M	6 Hrly
8	3248	FOG FRACTION AT 1.5 M	6 Hrly
9	4201	LARGE SCALE RAIN AMOUNT KG/M2/TS	6 Hrly
10	4202	LARGE SCALE SNOW AMOUNT KG/M2/TS	6 Hrly
11	5201	CONVECTIVE RAIN AMOUNT KG/M2/TS	6 Hrly
12	5202	CONVECTIVE SNOW AMOUNT KG/M2/TS	6 Hrly
13	9203	LOW CLOUD AMOUNT	6 Hrly
14	9204	MEDIUM CLOUD AMOUNT	6 Hrly
15	9205	HIGH CLOUD AMOUNT	6 Hrly
16	9210	CLOUD BASE ASL COVER.GT.2.5 OCTA KFT	6 Hrly
17	9217	TOTAL CLOUD AMOUNT MAX/RANDOM OVERLP	6 Hrly
18	15201	U WIND ON PRESSURE LEVELS B GRID	6 Hrly
19	15202	V WIND ON PRESSURE LEVELS B GRID	6 Hrly
20	16202	GEOPOTENTIAL HEIGHT ON P LEV/P GRID	6 Hrly
21	16203	TEMPERATURE ON P LEV/P GRID	6 Hrly
22	16204	RH WRT ICE ON P LEV/P GRID	6 Hrly
23	16222	PRESSURE AT MEAN SEA LEVEL	6 Hrly
24	16256	RH WRT WATER ON P LEV/P GRID	6 Hrly

Fields in file cplhca_pb000

Sl No.	STASH Code	Field Name	Frequency
1	2	U COMPNT OF WIND AFTER TIMESTEP	Daily
2	3	V COMPNT OF WIND AFTER TIMESTEP	Daily
3	10	SPECIFIC HUMIDITY AFTER TIMESTEP	Daily
4	24	SURFACE TEMPERATURE AFTER TIMESTEP	Daily
5	150	W COMPNT OF WIND AFTER TIMESTEP	Daily
6	409	SURFACE PRESSURE AFTER TIMESTEP	Daily

7	1201	NET DOWN SURFACE SW FLUX: SW TS ONLY	Daily
8	1203	NET DN SW RAD FLUX:OPEN SEA:SEA MEAN	Daily
9	1207	INCOMING SW RAD FLUX (TOA): ALL TSS	Daily
10	1208	OUTGOING SW RAD FLUX (TOA)	Daily
11	1209	CLEAR-SKY (II) UPWARD SW FLUX (TOA)	Daily
12	1210	CLEAR-SKY (II) DOWN SURFACE SW FLUX	Daily
13	1211	CLEAR-SKY (II) UP SURFACE SW FLUX	Daily
14	1235	TOTAL DOWNWARD SURFACE SW FLUX	Daily
15	2201	NET DOWN SURFACE LW RAD FLUX	Daily
16	2203	NET DN LW RAD FLUX:OPEN SEA:SEA MEAN	Daily
17	2205	OUTGOING LW RAD FLUX (TOA)	Daily
18	2206	CLEAR-SKY (II) UPWARD LW FLUX (TOA)	Daily
19	2207	DOWNWARD LW RAD FLUX: SURFACE	Daily
20	2208	CLEAR-SKY (II) DOWN SURFACE LW FLUX	Daily
21	3217	SURFACE SENSIBLE HEAT FLUX W/M2	Daily
22	3223	SURFACE TOTAL MOISTURE FLUX KG/M2/S	Daily
23	3234	SURFACE LATENT HEAT FLUX W/M2	Daily
24	3237	SPECIFIC HUMIDITY AT 1.5M	Daily
25	3298	SUBLIM. SURFACE (GBM) : RATE KG/M2/S	Daily
26	4203	LARGE SCALE RAINFALL RATE KG/M2/S	Daily
27	4204	LARGE SCALE SNOWFALL RATE KG/M2/S	Daily
28	5205	CONVECTIVE RAINFALL RATE KG/M2/S	Daily
29	5206	CONVECTIVE SNOWFALL RATE KG/M2/S	Daily
30	5216	TOTAL PRECIPITATION RATE KG/M2/S	Daily
31	9203	LOW CLOUD AMOUNT	Daily
32	9204	MEDIUM CLOUD AMOUNT	Daily
33	9205	HIGH CLOUD AMOUNT	Daily
34	15214	ERTEL POTENTIAL VORTICITY THETA SURF	Daily
35	30428	dry mass col int u*q per unit area	Daily
36	30429	dry mass col int v*q per unit area	Daily

Fields in file cplhca_pc000

Sl No.	**STASH Code**	**Field Name**	**Frequency**

Fields in file cplhca_pd000

Sl No.	STASH Code	Field Name	Frequency
1	2205	OUTGOING LW RAD FLUX (TOA)	3 Hrly
2	5216	TOTAL PRECIPITATION RATE KG/M2/S	3 Hrly
3	5226	TOTAL PRECIPITATION AMOUNT KG/M2/TS	3 Hrly
4	15201	U WIND ON PRESSURE LEVELS B GRID	3 Hrly
5	15202	V WIND ON PRESSURE LEVELS B GRID	3 Hrly

Fields in file cplhca_pe000

Sl No.	STASH Code	Field Name	Frequency
1	30201	U COMPNT OF WIND ON P LEV/UV GRID	Daily
2	30202	V COMPNT OF WIND ON P LEV/UV GRID	Daily
3	30204	TEMPERATURE ON P LEV/UV GRID	Daily
4	30207	GEOPOTENTIAL HEIGHT ON P LEV/UV GRID	Daily
5	30208	OMEGA ON P LEV/UV GRID	Daily
6	30211	UU ON P LEV/UV GRID	Daily
7	30212	UV ON P LEV/UV GRID	Daily
8	30214	UT ON P LEV/UV GRID	Daily
9	30218	UOM ON P LEV/UV GRID	Daily
10	30222	VV ON P LEV/UV GRID	Daily
11	30224	VT ON P LEV/UV GRID	Daily
12	30228	VOM ON P LEV/UV GRID	Daily
13	30244	TT ON P LEV/UV GRID	Daily
14	30248	TOM ON P LEV/UV GRID	Daily
15	30288	OMOM ON P LEV/UV GRID	Daily
16	30301	HEAVYSIDE FN ON P LEV/UV GRID	Daily
17	30418	PSTAR UV GRID	Daily

Table B. 2: List of simulated variables for ocean model

Fields in file cplhco_foamdiurnal.grid_T.nc

Sl No.	Field Name	Units	Frequency
1	Depth Of Isosurface Of Sea Water Potential Temperature	m	1 Hrly
2	Downwelling Photosynthetic Radiative Flux In Sea Water	W/m2	1 Hrly
3	Integral Of Sea Water Potential Temperature Wrt Depth Expressed As Heat Content	J/m2	1 Hrly
4	Ocean Mixed Layer Thickness Defined By Sigma Theta	m	1 Hrly
5	Sea Surface Height Above Geoid	m	1 Hrly
6	Sea Surface Salinity	PSU	1 Hrly
7	Sea Surface Temperature	degC	1 Hrly
8	Surface Downward Heat Flux In Sea Water	W/m2	1 Hrly
9	Water Flux Out Of Sea Ice And Sea Water	kg/m2/s	1 Hrly

Fields in file cplhco_foamdiurnal.grid_U.nc

Sl No.	Field Name	Units	Frequency
1	Surface Downward X Stress	N/m2	1 Hrly

Fields in file cplhco_foamdiurnal.grid_V.nc

Sl No.	Field Name	Units	Frequency
1	Surface Downward Y Stress	N/m2	1 Hrly

Fields in file cplhco_foamlite.grid_T.nc

Sl No.	Field Name	Units	Frequency
1	Ocean Mixed Layer Thickness Defined By Sigma Theta	m	3 Hrly
2	Sea Surface Height Above Geoid	m	3 Hrly
3	Sea Surface Salinity	PSU	3 Hrly
4	Sea Surface Temperature	degC	3 Hrly
5	Temperature At 1.56M	degC	3 Hrly
6	Temperature At 11.77M	degC	3 Hrly
7	Temperature At 2.67M	degC	3 Hrly
8	Temperature At 3.86M	degC	3 Hrly
9	Temperature At 5.14M	degC	3 Hrly
10	Temperature At 6.54M	degC	3 Hrly
11	Temperature At 8.09M	degC	3 Hrly
12	Temperature At 9.82M	degC	3 Hrly

Fields in file cplhco_foamlite.grid_U.nc

Sl No.	Field Name	Units	Frequency
1	Ocean Current Along I-Axis: Surface	m/s	3 Hrly

Fields in file cplhco_foamlite.grid_V.nc

Sl No.	Field Name	Units	Frequency
1	Ocean Current Along J-Axis: Surface	m/s	3 Hrly

Fields in file cplhco_mersea.grid_T.nc

Sl No.	Field Name	Units	Frequency
1	Downwelling Photosynthetic Radiative Flux In Sea Water	W/m2	Daily
2	Liquid Precipitation	kg/m2/s	Daily
3	Mixed Layer Depth |Dt|=0.2 (Ref.10M)	m	Daily
4	Ocean Mixed Layer Thickness Defined By Sigma Theta	m	Daily
5	Ocean Mixed Layer Thickness Defined By Vertical Tracer Diffusivity	m	Daily
6	Sea Surface Height Above Geoid	m	Daily
7	Sea Water Potential Temperature	degC	Daily
8	Sea Water Salinity	PSU	Daily
9	Snow Precipitation	kg/m2/s	Daily
10	Surface Downward Heat Flux In Sea Water	W/m2	Daily
11	Water Flux Into Sea Water From Rivers	kg/m2/s	Daily
12	Water Flux Out Of Sea Ice And Sea Water	kg/m2/s	Daily

Fields in file cplhco_mersea.grid_U.nc

Sl No.	Field Name	Units	Frequency

1	Sea Water X Velocity	m/s	Daily
2	Surface Downward X Stress	N/m2	Daily

Fields in file cplhco_mersea.grid_V.nc

Sl No.	Field Name	Units	Frequency
1	Sea Water Y Velocity	m/s	Daily
2	Surface Downward Y Stress	N/m2	Daily

Table B. 3: List of simulated variables for sea-ice model

Sl No.	Field Name	Units	Frequency
1	Area Tendency Dynamics	%/day	Daily
2	Area Tendency Thermo	%/day	Daily
3	Atm/Ice Stress (X)	N/m^2	Daily
4	Atm/Ice Stress (Y)	N/m^2	Daily
5	Basal Ice Melt	cm/day	Daily
6	Compressive Ice Strength	N/m	Daily
7	Congelation Ice Growth	cm/day	Daily
8	Coriolis Stress (X)	N/m^2	Daily
9	Coriolis Stress (Y)	N/m^2	Daily
10	Evaporative Water Flux	cm/day	Daily
11	Frazil Ice Growth	cm/day	Daily
12	FreshwtrFlx Ice To Ocn	cm/day	Daily
13	Grid Cell Mean Ice Thickness	M	Daily
14	Grid Cell Mean Snow Thickness	M	Daily
15	Heat Flux Ice To Ocean	W/m^2	Daily
16	Ice Area (Aggregate)	1	Daily
17	Ice Area, Categories	1	Daily
18	Ice Velocity (X)	m/s	Daily
19	Ice Velocity (Y)	m/s	Daily
20	Ice Volume, Categories	M	Daily
21	Internal Ice Stress (X)	N/m^2	Daily
22	Internal Ice Stress (Y)	N/m^2	Daily
23	Latent Heat Flux	W/m^2	Daily
24	Lateral Ice Melt	cm/day	Daily
25	Net Sfc Heat Flux Causing Melt, Cat	W/m^2	Daily
26	Net Surface Heat Flux	W/m^2	Daily
27	Net Surface Heat Flux Causing Melt	W/m^2	Daily
28	Net Surface Heat Flux, Categories	W/m^2	Daily
29	Ocean/Ice Stress (X)	N/m^2	Daily
30	Ocean/Ice Stress (Y)	N/m^2	Daily
31	Salt Flux Ice To Ocean	kg/m^2/s	Daily
32	Sea Sfc Tilt Stress (X)	N/m^2	Daily
33	Sea Sfc Tilt Stress (Y)	N/m^2	Daily
34	Snow-Ice Formation	cm/day	Daily

35	Snowfall Rate	cm/day	Daily
36	Top Ice Melt	cm/day	Daily
37	Top Sfc Conductive Heat Flux, Cat	W/m^2	Daily
38	Top Snow Melt	cm/day	Daily
39	Top Surface Conductive Heat Flux	W/m^2	Daily
40	Volume Tendency Dynamics	cm/day	Daily
41	Volume Tendency Thermo	cm/day	Daily